Sonography of the Scalp and Hair

19

Ximena Wortsman and Jacobo Wortsman

Contents

19.1 Introduction

Scalp hair is traditionally considered a conveyor of self image, identity, ethnicity, and health [1, 2]. Understandably, pathologies affecting the scalp, and hence scalp hair, frequently result in serious impacts on the quality of life. Improvement in scalp appearance and hair density are the main goals of cosmetic products and plastic surgery hair restoration procedures. Physiological studies have shown that adult body hair is not homogeneous, but rather it is subject to remarkable interregional differences. For example, eyelashes are structurally similar to scalp hair, but differ notably in the distribution of the mitotically active K-19 positive stem cells reservoirs that are distributed along the outer root sheath (ORS) of eyelash follicles, but are separated into two ORS reservoirs in the upper and lower third of scalp hair. Also, the human gene dopachrome tautomerase, involved in melanin synthesis, is expressed only in eyelash melanocytes, being strikingly absent in scalp hair melanocytes. Finally, the hair cycle is shorter in eyelashes than scalp hair [3].

In this chapter we will discuss the potential of ultrasound in the evaluation of diseases of the scalp and the corresponding structural changes in scalp hair.

19.2 Technical Considerations

The sonographer should face the lesion site(s) directly; a copious amount of gel is applied over the scalp and the hair tracts are displaced to the borders of the lesion site; testing (grey scale and color Doppler ultrasound with spectral curve analysis) routinely includes panoramic scalp readings obtained along at least the two main perpendicular axes (transverse and longitudinal), while hair follicles are followed along their main axis and also on two perpendicular views. Hair tracts can better be observed after trimming and being embedded in saline in a small plastic receptacle. The use of stand-off pads or contrast medium is usually not necessary in baseline studies [4].

X. Wortsman, MD (✉)
Department of Radiology and Dermatology,
Institute for Diagnostic Imaging
and Research of the Skin and Soft Tissues, Clinica Servet,
Faculty of Medicine, University of Chile, Almirante Pastene 150,
Providencia, Santiago, Chile
e-mail: xwo@tie.cl, xworts@yahoo.com, www.sonoskin.com

J. Wortsman, MD
Department of Medicine,
Southern Illinois University School of Medicine,
3128 Temple Drive, Springfield, IL 62704, USA

X. Wortsman, G.B.E. Jemec (eds.), *Dermatologic Ultrasound with Clinical and Histologic Correlations*,
DOI 10.1007/978-1-4614-7184-4_19,

19.3 Sonographic Anatomy of Scalp Skin

The skin of the scalp maintains the echostructure already described for other corporal segments [5], the frontal skin being thinner than the occipital skin [6]; therefore, the epidermis appears as a hyperechoic line; the dermis, as a hyperechoic band; and the subcutaneous tissue, as a hypoechoic band. A thin hypoechoic band seen under the subcutaneous tissue corresponds to the epicranius muscle or galeal layer (i.e. the epicranius muscle and its aponeurosis), and a deeper hyperechoic line marks the bony margin of the skull. The blood supply to the scalp comes from a centripetal network, with larger trunks running subcutaneously in the periphery and reaching the midline through branches of the external and internal carotid arteries [6].

The longitudinal structure of the hair follicle includes the dermal follicle bulb most proximally and the hair tract (shaft) more proximally, and their position within the scalp depends on rhythmic growth cycles (the "hair cycle clock") [7], for example, the telogen or resting phase when the hair bulb is in a superficial subdermal location; the anagen or active growth phase with a deeply located hair bulb almost in the subcutaneous tissue; and the catagen or transition phase, between the telogen and anagen. The growth cycle independently affects each individual follicle and therefore, human hairs are not shed simultaneously as in the case of many animals. Normally, 90 % of scalp hairs are in the anagen phase, and the remaining 10 % are in the telogen and catagen phases [4, 8] (Figs. 19.1, 19.2, 19.3, 19.4, 19.5, 19.6, 19.7, and 19.8).

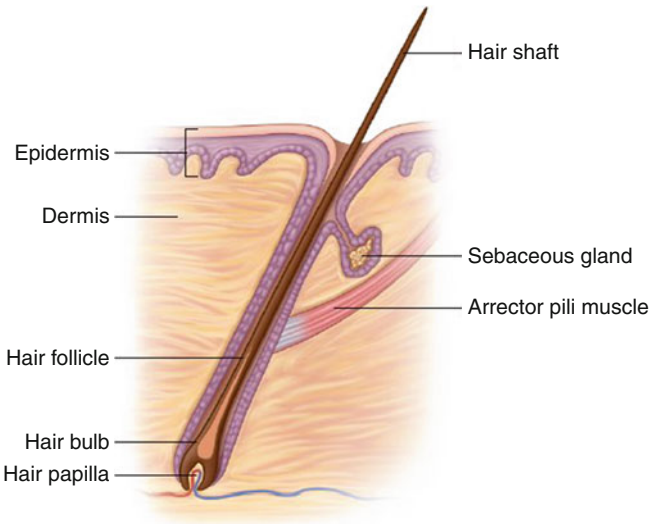

Fig. 19.1 Drawing of the anatomy of the hair follicle and tract

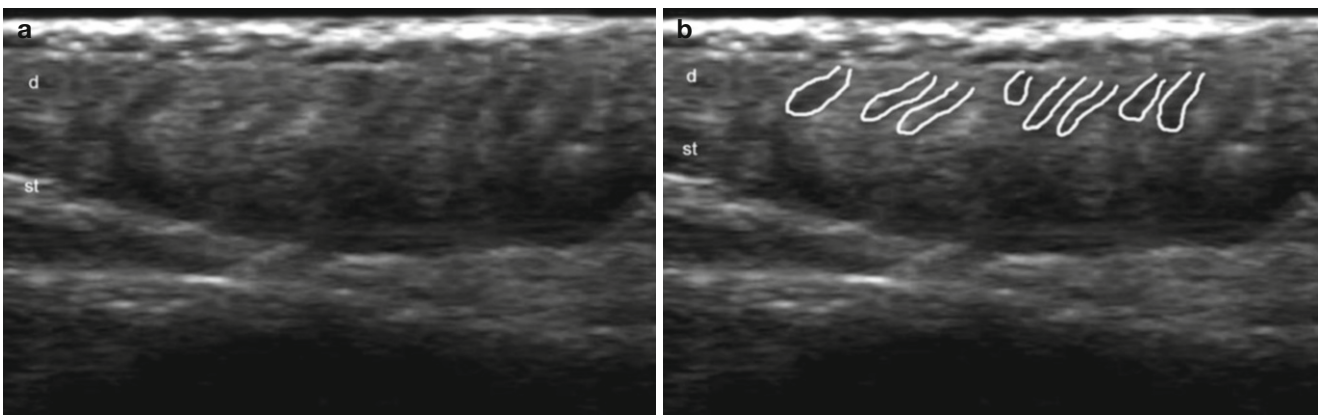

Fig. 19.2 (**a**–**d**) Sonoanatomy of the scalp and hair follicles (occipital region). (**a**, **b**) Grey scale ultrasound images (scalp); (**b**) with the hair follicles outlined. (**c**, **d**) 3D reconstructions of the hair follicles (axilla); (**d**) with the hair follicles outlined. *Abbreviations*: *d* dermis, *st* subcutaneous tissue

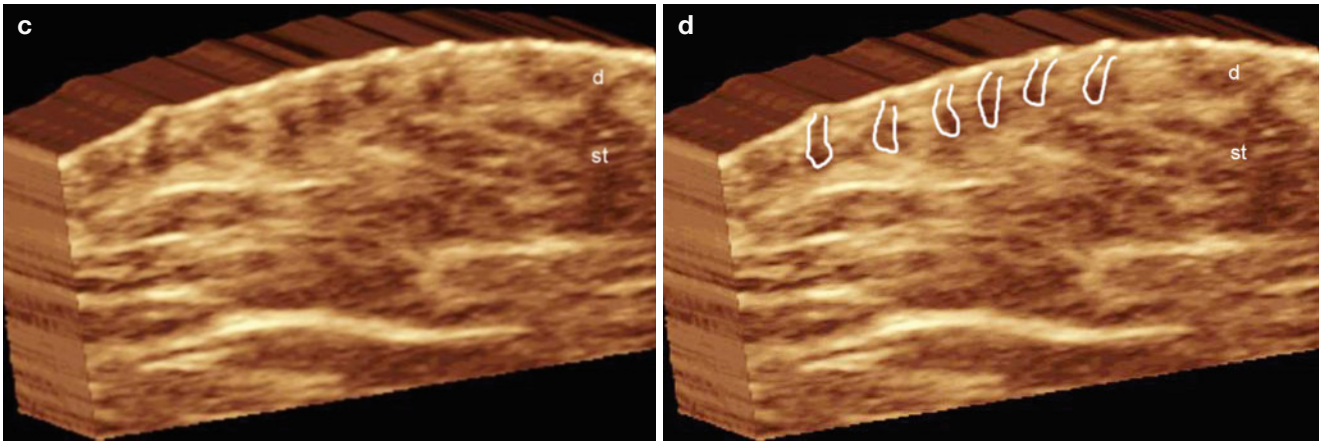

Fig. 19.2 (continued)

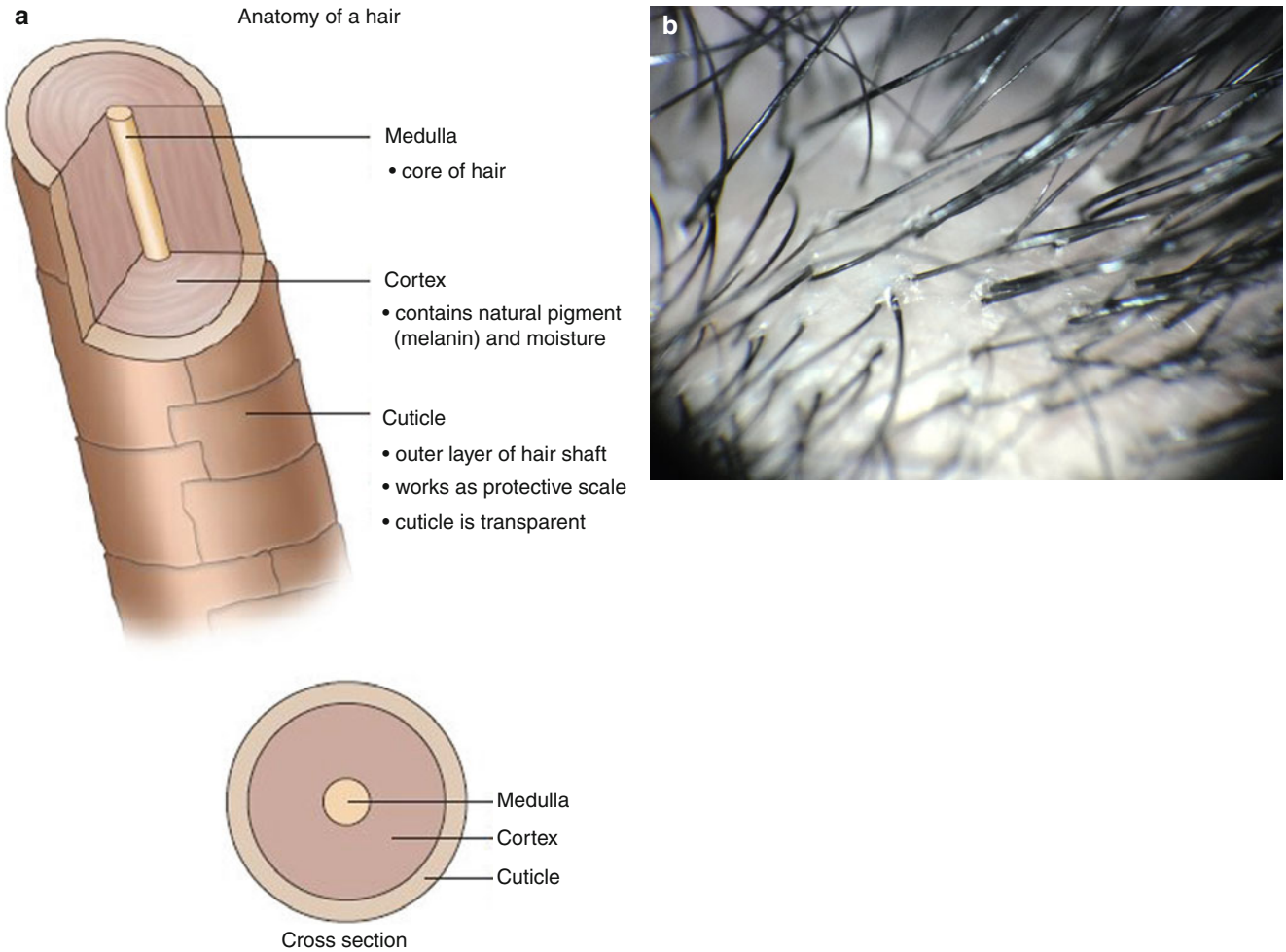

Fig. 19.3 (**a**–**e**) Hair tract. (**a**) Anatomical drawing of the parts of a hair tract. (**b**) Dermoscopy image of the hair tracts in the scalp. (**c**) Sonoanatomy of the hair tract (grey scale). (**d**) Sweep electron microscope image of a hair tract shows the cuticle layer. (**e**) Histology (HE ×25 zoom, courtesy of Dr. Laura Carreño): skin of the scalp shows mature hair follicles (*arrows*). The bulbs (base) of the hair follicles (*arrows*) anchor in the upper subcutaneous tissue

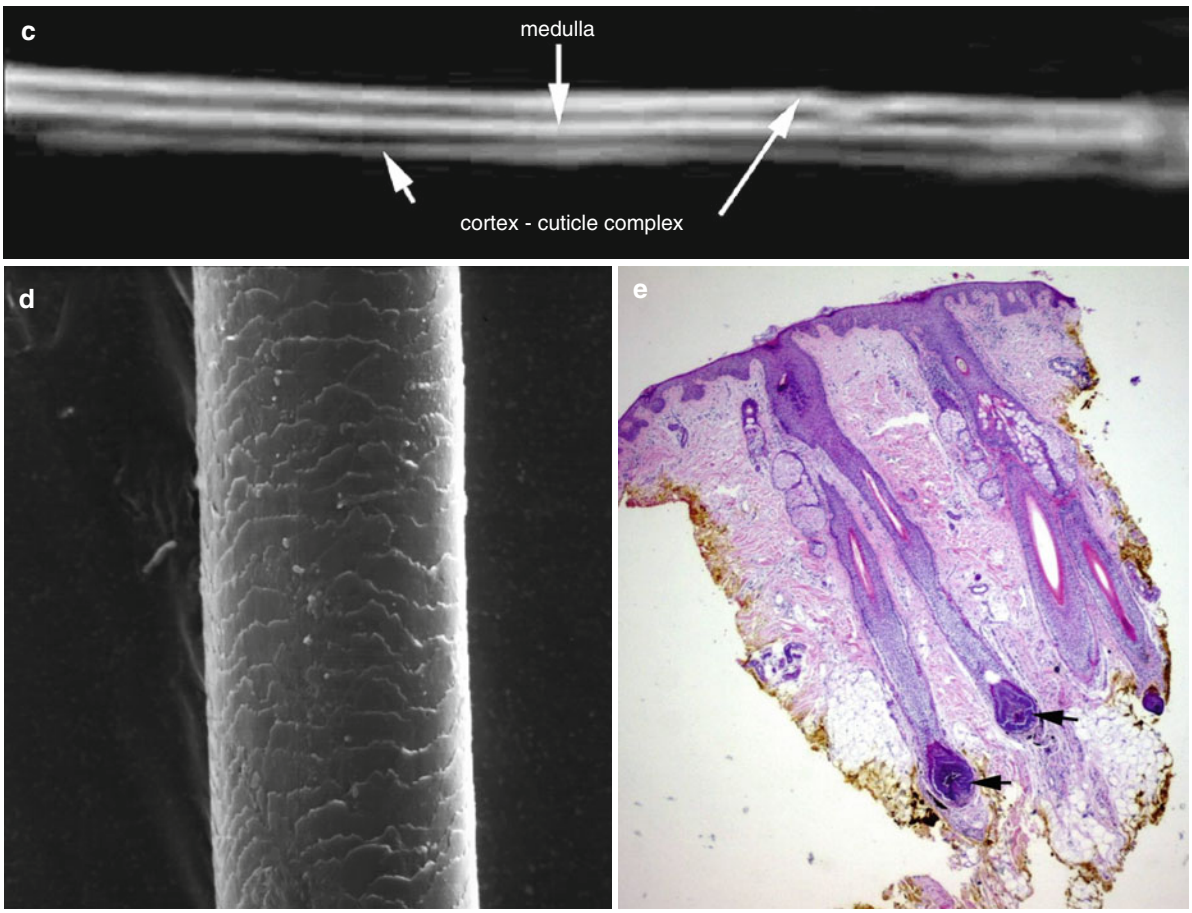

Fig. 19.3 (continued)

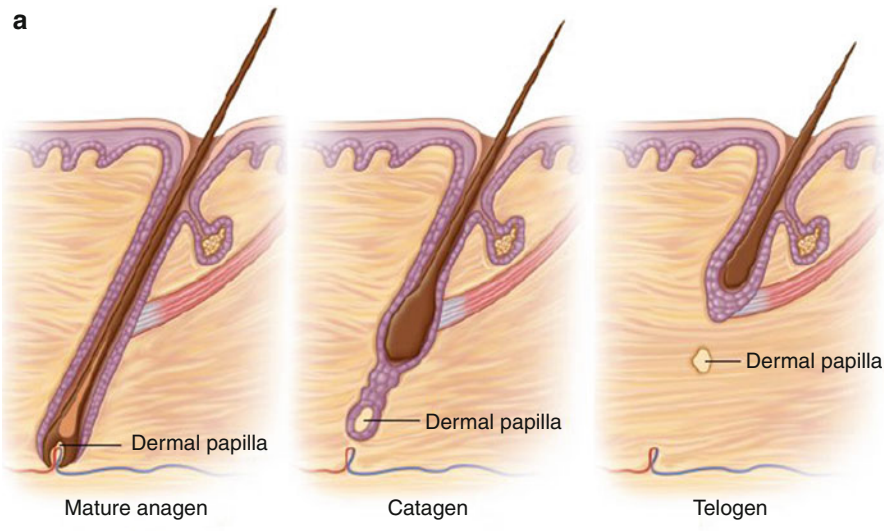

Fig. 19.4 (**a**, **b**) Hair follicle cycle. (**a**) Drawing. (**b**) Histology (HE ×25 zoom, courtesy of Dr. Laura Carreño): shows immature (*arrowheads*) and mature (*arrows*) hair follicles

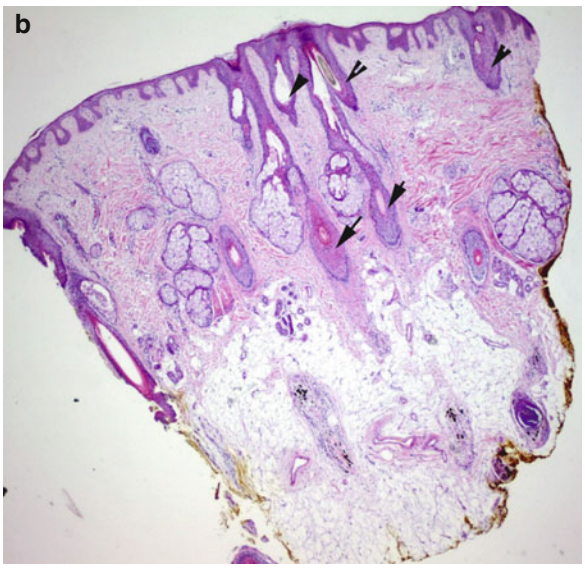

Fig. 19.4 (continued)

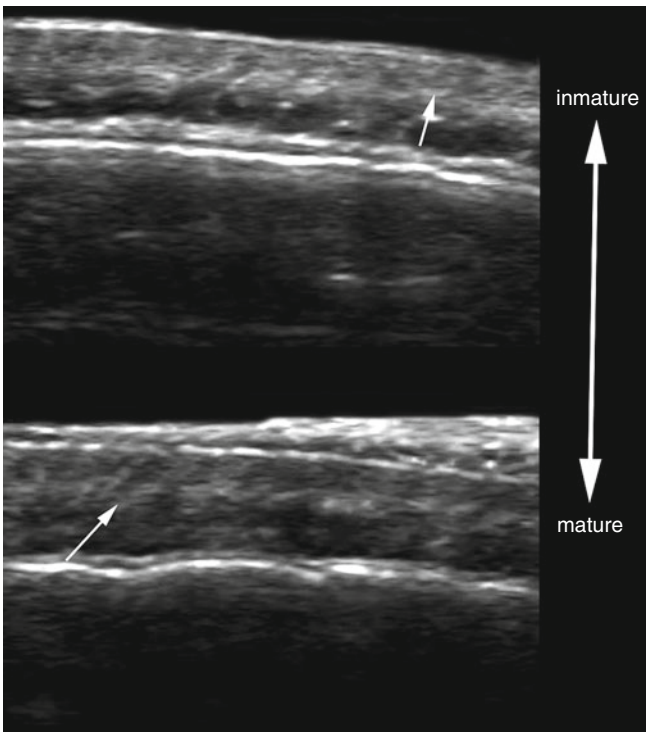

Fig. 19.5 Grey scale image showing sonographic appearance of the hair follicle cycle. The arrows show the location of the hair follicles in the dermis

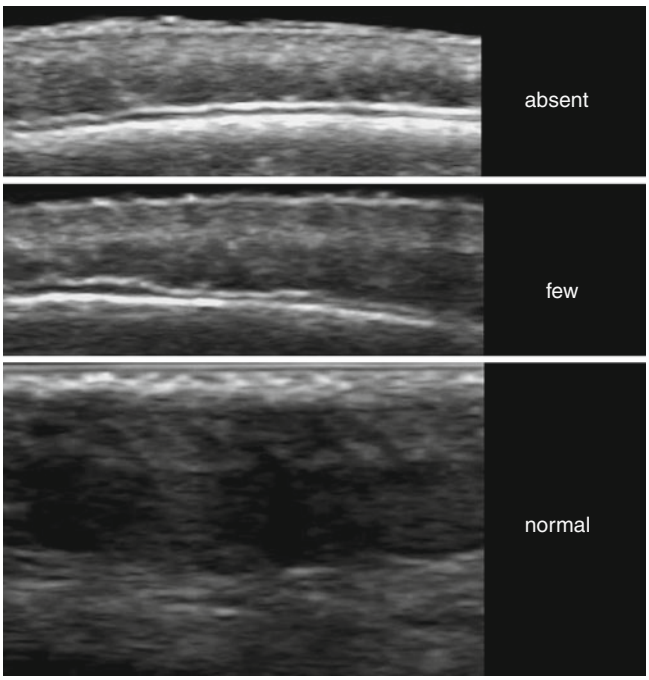

Fig. 19.6 Grey scale image showing sonographic grading of the density of the hair follicles in the scalp

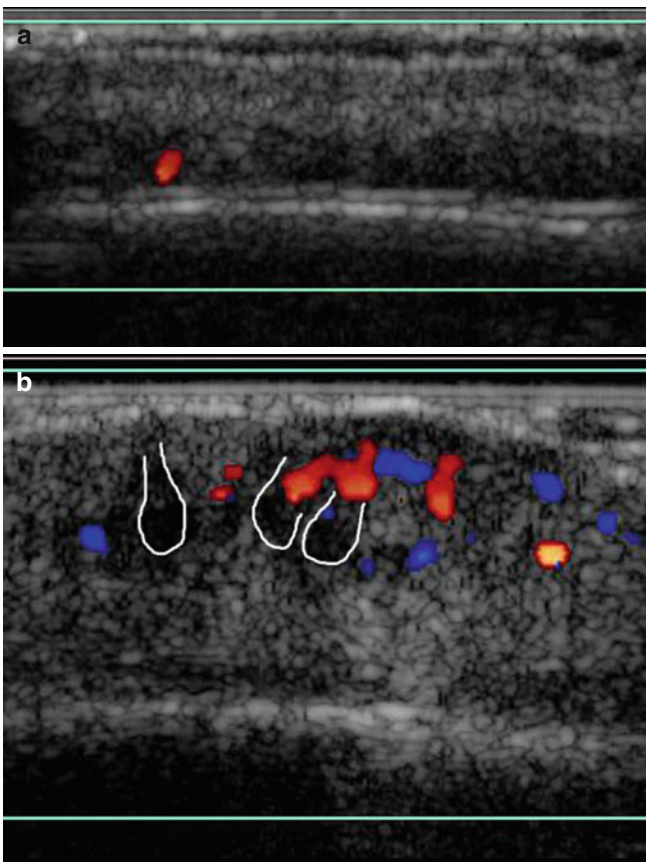

Fig. 19.7 (**a**, **b**) Color Doppler sonographic image showing grading of vascularity of the scalp. (**a**) Normal. (**b**) Increased (hair follicles outlined)

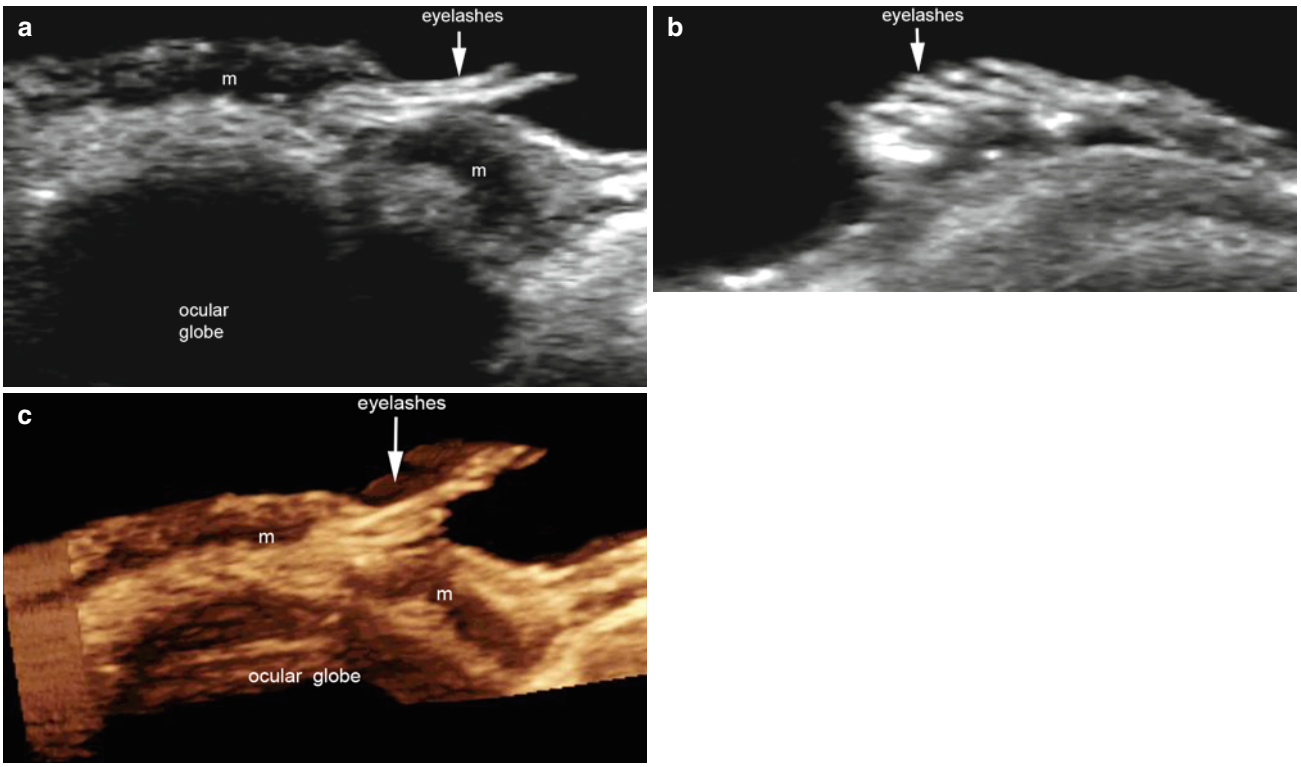

Fig. 19.8 (**a**–**c**) Eyelashes (*arrows*). (**a**, **b**) Grey scale ultrasound images (**b** longitudinal view; **c** transverse view). (**c**) 3D reconstruction (longitudinal view; 5–8 s sweep). *Abbreviations*: *m* orbicularis muscle of the eyelid

19.4 Sonographic Anatomy of the Hair Tract

Histologically, the hair tract (shaft) consists of an outer sheath, comprising the complex cuticle-cortex and an inner central medulla. In recent imaging studies using experimental magnetic resonance imaging machines, the same morphology has been observed with clear separation of the cortex and medulla [9]. Ultrasound provides additional structural details because scalp hair shafts from the scalp mainly present a trilaminar hyperechoic structure presumably reflecting the longitudinal arrangement of the keratin chains. This structure resembles the sonographic bilaminar appearance of another keratinized organ, the ungual plaque of the nail [10]. The trilaminar organization of scalp hair tracts is nevertheless unique because the eyelashes are uniformly monolaminar. It is not clear if the eyelashes present this appearance because of the current limitations in the resolution of ultrasound machines or whether this represents a true morphology of the keratinous component [4] (Figs. 19.3 and 19.8).

19.5 Hair Follicle Quantification

Ultrasound provides a qualitative estimation of the density of scalp hair follicles from their total absence, in alopecia or post-chemotherapy status, to a reduction in follicle number; thus, ultrasound detects not only abnormalities in the actual appearance of the hair follicles, but also alterations of the local hair growth cycle, properties clinically helpful in comprehensive monitoring of treatments directed at correcting baldness [4] (Fig. 19.6).

19.6 Hair Follicle Inflammation

Hair follicle inflammation, also called folliculitis, implies an active inflammatory process within the hair follicle itself or in the surrounding tissues that produces changes in hair follicle diameter and/or echogenicity. Thus, the follicle is both swollen and markedly hypoechoic in the presence of inflammation. Adding determination of the vascularity pattern by color Doppler ultrasound can further show increased blood flow, another sign of inflammation [4] (Fig. 19.7)

19.7 Disorders of Scalp Skin and Scalp Hair

19.7.1 Benign Conditions

19.7.1.1 Trichilemmal Cyst

Trichilemmal cysts (TCs) are cystic structures originating from the trichilemma or exposed outer root of the hair sheath. TCs are thought to be derived from the isthmus of the hair follicle (the zone between hair bulb and hair shaft), and comprise approximately 20 % of epithelial cysts (the remaining 80 % is represented by epidermis-derived, epidermal cysts), with the most common locations being the scalp (78 %) and torso (13 %) [11]. TCs present clinically as smooth, firm nodules often accompanied by hair loss. Histologically, TC is typically seen as a sharply circumscribed cystic wall with abrupt transition between the epidermal stratum spinosum and hair keratin, without the intervening granular layer. The cysts often contain keratinous debris and cholesterol crystals from keratin liquefaction, and occasional focal calcifications and trapped hair tracts [12, 13]. Sonography of TCs usually presents as anechoic or hypoechoic round or oval-shaped structures in the dermis and subcutaneous tissue, usually without connecting tracts to the epidermal layer. Detectable echoes within the cyst generally correspond to keratinous and dense cholesterol elements [4]. TCs can occasionally present as target nodules with a hypoechoic rim and heterogeneous center that contains hyperechoic lines that correspond to hair tracts fragments. In contrast to the calcium deposits that are seen in the "target nodule" sonographic appearance of pilomatrixomas, the hyperechoic hair fragments tend to not present posterior acoustic shadowing artifact (Figs. 19.9, 19.10, 19.11, and 19.12).

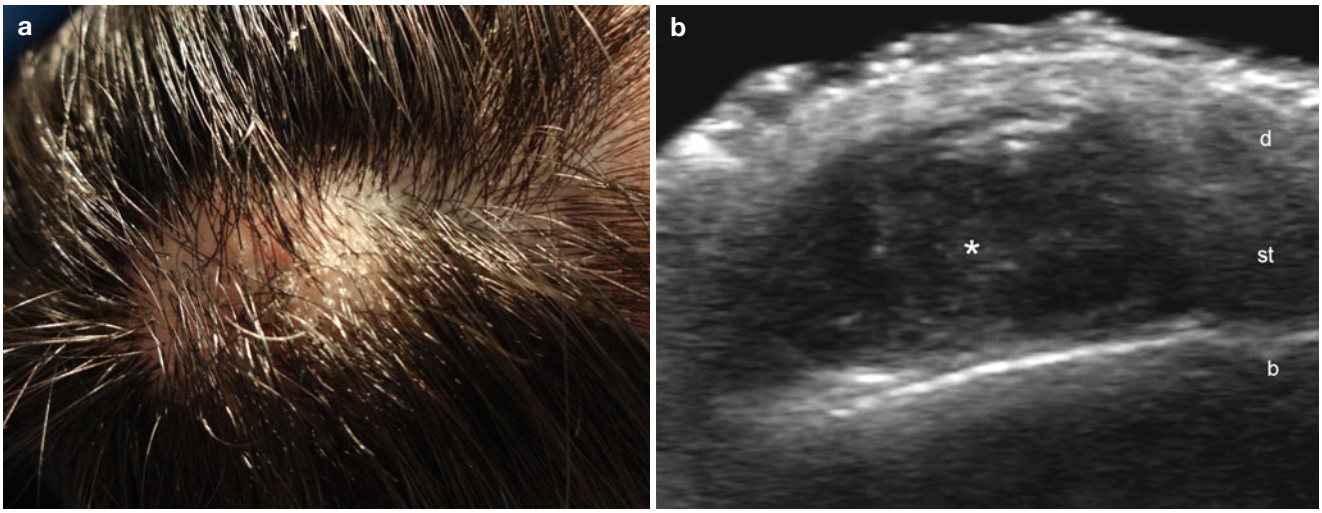

Fig. 19.9 (**a**–**e**) Trichilemmal cyst. (**a**) Clinical photograph shows focal alopecia and swelling. (**b**) Grey scale ultrasound image (longitudinal view; frontal scalp) demonstrates a well-defined, oval-shaped, anechoic structure (*) that presents echoes (debris) and is located in the dermis and subcutaneous tissue. (**c**) Color Doppler ultrasound image (longitudinal view; frontal scalp) demonstrates a lack of vascularity within the cyst. (**d**) 3D reconstruction of the cyst (*). (**e**) Histology (HE ×100 zoom, courtesy of Dr. Claudia Morales) shows compact keratin in the lumen of the cyst. The cyst is lined by epithelium without a granular layer. *Abbreviations*: *d* dermis, *st* subcutaneous tissue, *b* bony margin of the skull, *k* keratin, *e* epithelium

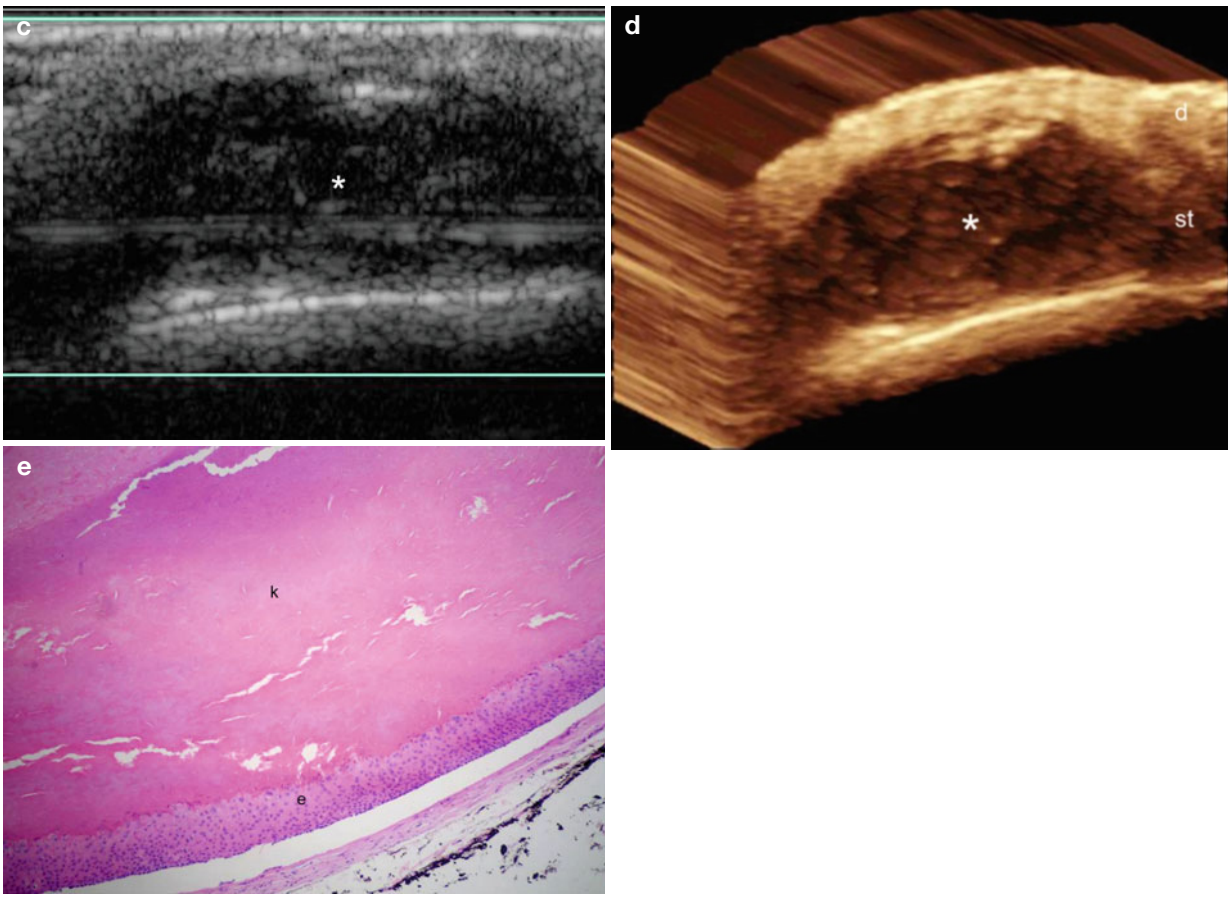

Fig. 19.9 (continued)

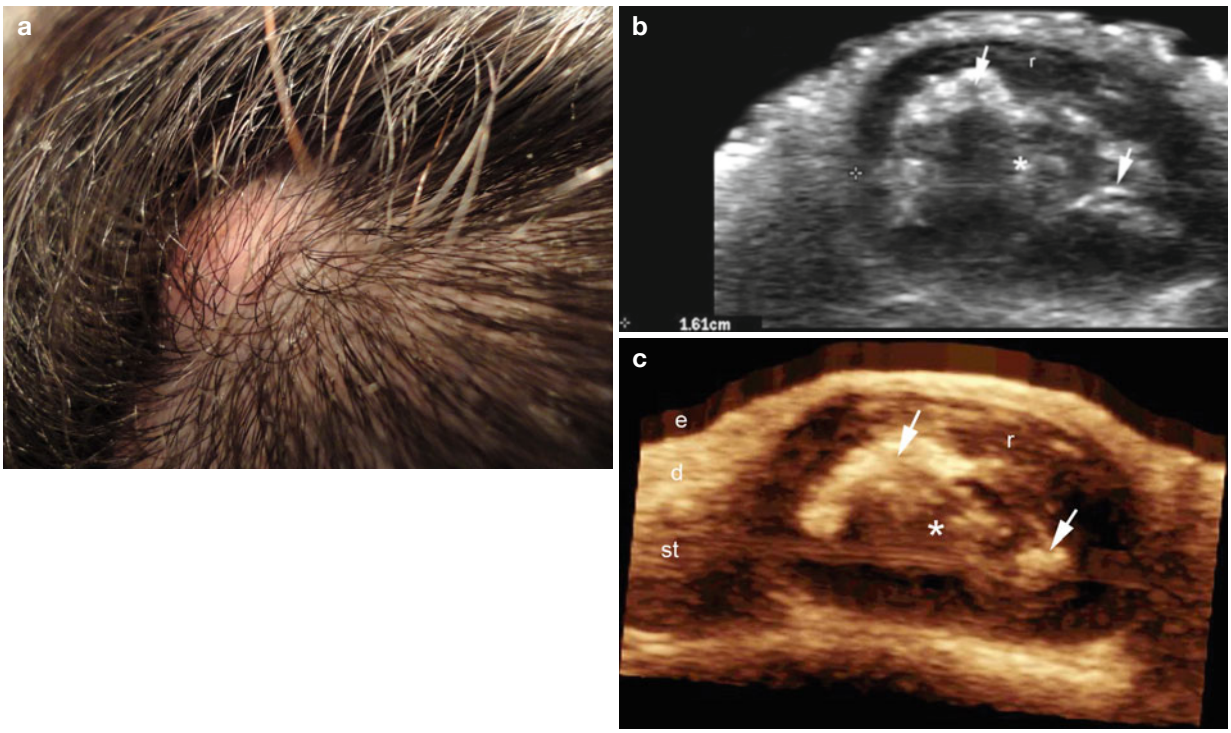

Fig. 19.10 (**a**–**c**) Trichilemmal cyst. (**a**) Clinical image shows swelling and focal alopecia. (**b**, **c**) Grey scale ultrasound images (**b** 2D and **c** 3D; transverse view, left parietal region) demonstrate a 1.61 cm well-defined, oval-shaped nodule that presents a hypoechoic rim (*r*) and heterogeneous center (*). Notice the hyperechoic lines in the center that correspond to trapped hair tracts fragments (*arrows*). *Abbreviations*: *e* epidermis, *d* dermis, *st* subcutaneous tissue

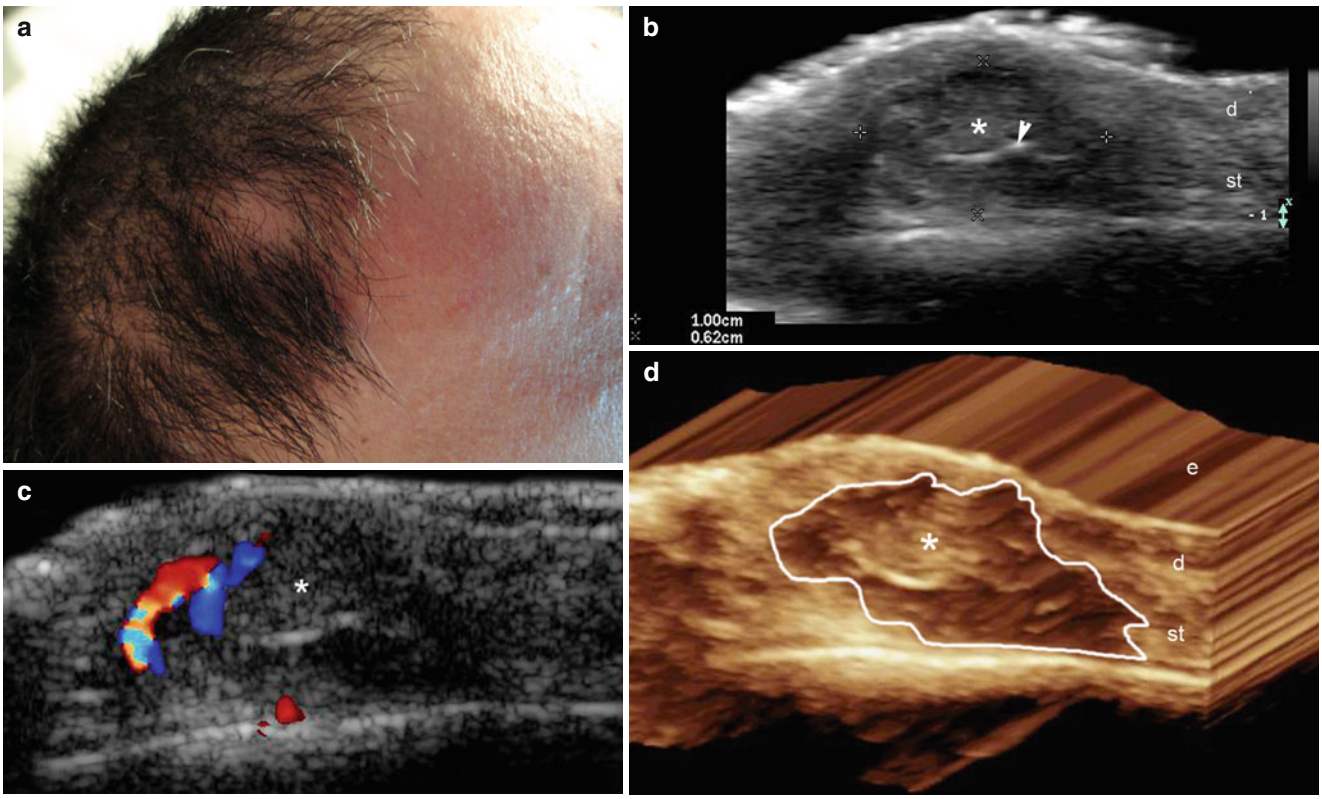

Fig. 19.11 (**a**–**d**) Trichilemmal cyst. (**a**) Clinical photograph demonstrates focal alopecia. (**b**) Grey scale ultrasound image (longitudinal view; right frontal region) shows a 1.0 cm (long)×0.62 cm (depth) well-defined oval-shaped hypoechoic structure (*, between markers) located in the dermis and subcutaneous tissue. Notice the fragment of hair tract (*arrowhead*) within the cyst. (**c**) Color Doppler ultrasound image (longitudinal view) demonstrates a mildly increased vascularity in the periphery of the cyst . (**d**) 3D reconstruction (longitudinal view, 5–8 s sweep) of the cyst (*, outlined). *Abbreviations*: *e* epidermis, *d* dermis; *st* subcutaneous tissue

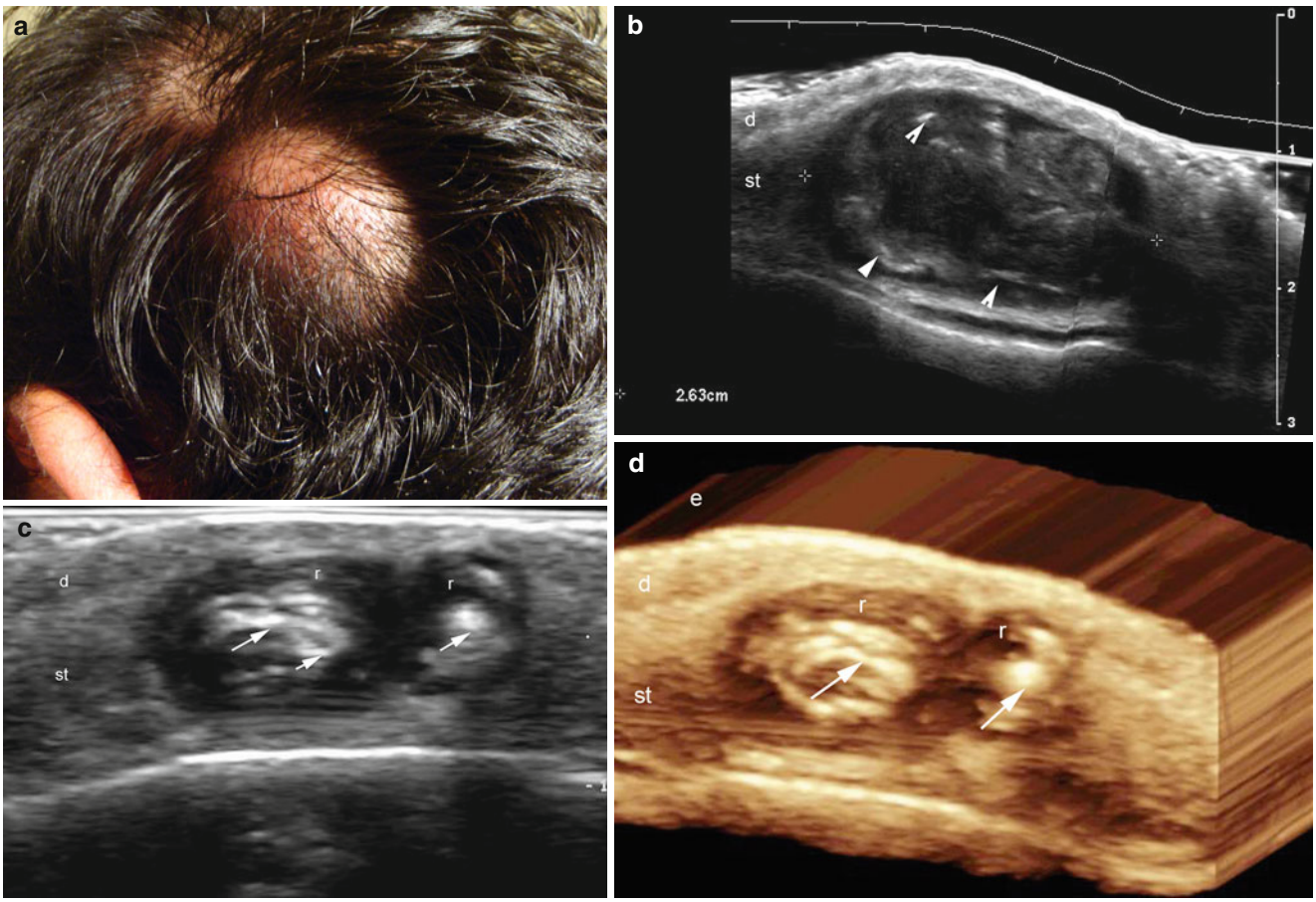

Fig. 19.12 (**a**–**d**) Multiple trichilemmal cysts. (**a**) Clinical photograph demonstrates a lump with focal alopecia. (**b**) Grey scale ultrasound image (longitudinal view) shows a 2.63 cm (long) well-defined oval-shaped hypoechoic and heterogeneous structure (between markers) in the subcutaneous tissue. Notice the hyperechoic lines that correspond to hair tracts fragments (*arrowheads*). (**c**, **d**) Grey scale ultrasound images (**b** 2D longitudinal view and **c** 3D reconstruction in same patient) show two additional well-defined oval-shaped structures that present hypoechoic rim (*r*) and heterogeneous center with hyperechoic lines that represent trapped hair tracts (*arrows*). *Abbreviations*: *e* epidermis, *d* dermis, *st* subcutaneous tissue

19.7.1.2 Pilomatrixoma

Pilomatrixoma, also known as pilomatricoma or calcifying epithelioma of Malherbe, is a benign tumor arising from the hair follicle matrix. Pilomatrixomas are most frequently found in children and young adults, especially in the head and neck, with 9 % of them located in the scalp [14]. The tumor often goes unrecognized until the time of surgery because of the non-specific clinical history of a painless, irregular, slowly enlarging hard nodule [15, 16]. Clinically, pilomatrixomas may also cause focal baldness in the scalp. Sonography of typical pilomatrixomas commonly shows a target-like lesion with a hyperechoic center and hypoechoic rim; hyperechoic dots are commonly seen within the nodule and correspond to calcium deposits. According to the size of the calcium deposits, a posterior acoustic shadowing can be detected [4, 17, 18] (Fig.19.13).

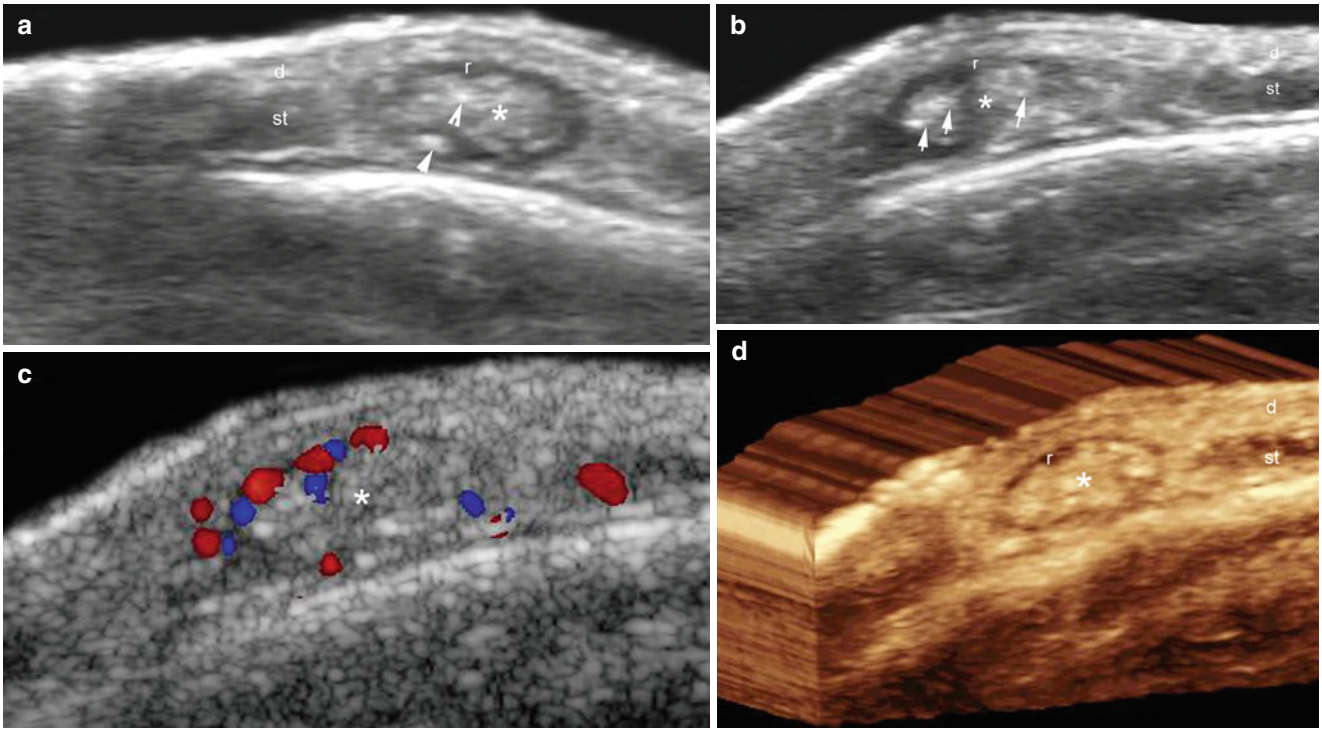

Fig. 19.13 (**a**–**d**) Pilomatrixoma. (**a**, **b**) Grey scale ultrasound images (**a** transverse view and **b** longitudinal view) demonstrate a target-like nodule that presents a hypoechoic rim (r) and a hyperechoic center (*) with hyperechoic spots (*arrows*) that correspond to calcium deposits. (**c**) Color Doppler ultrasound image (longitudinal view) shows increased vascularity in the periphery of the nodule. (**d**). 3D reconstruction (longitudinal view) highlights the lesion (*). *Abbreviations*: *d* dermis, *st* subcutaneous tissue, *r* rim

19.7.1.3 Hemangioma

Hemangiomas of infancy are the most common benign tumors of infancy, appearing shortly after birth in 5–10 % of infants. Clinically, many hemangiomas are discrete and well-circumscribed soft, reddish tumors of the head or neck; others are segmental and diffuse and often involve larger areas [19]. On sonography, hemangiomas present as ill-defined structures that can vary in their echogenicity according to the phase of activity. Thus, they show hypoechogenicity during the proliferative phase, and hyperechogenicity in the total regression phase. During the partial regression phase, hemangiomas can appear as heterogeneous structures (i.e., mixed hyper- and hypoechoic areas). Hemangiomas present prominent arterial and venous vessels or arteriovenous shunts [4, 20, 21] in the proliferative phase and turn hypovascular in the total regression phase. Deep vascular tumoral involvement extending to the epicranius muscle or bony margins of the skull can occasionally be detected [22, 23] (Figs. 19.14, 19.15, and 19.16).

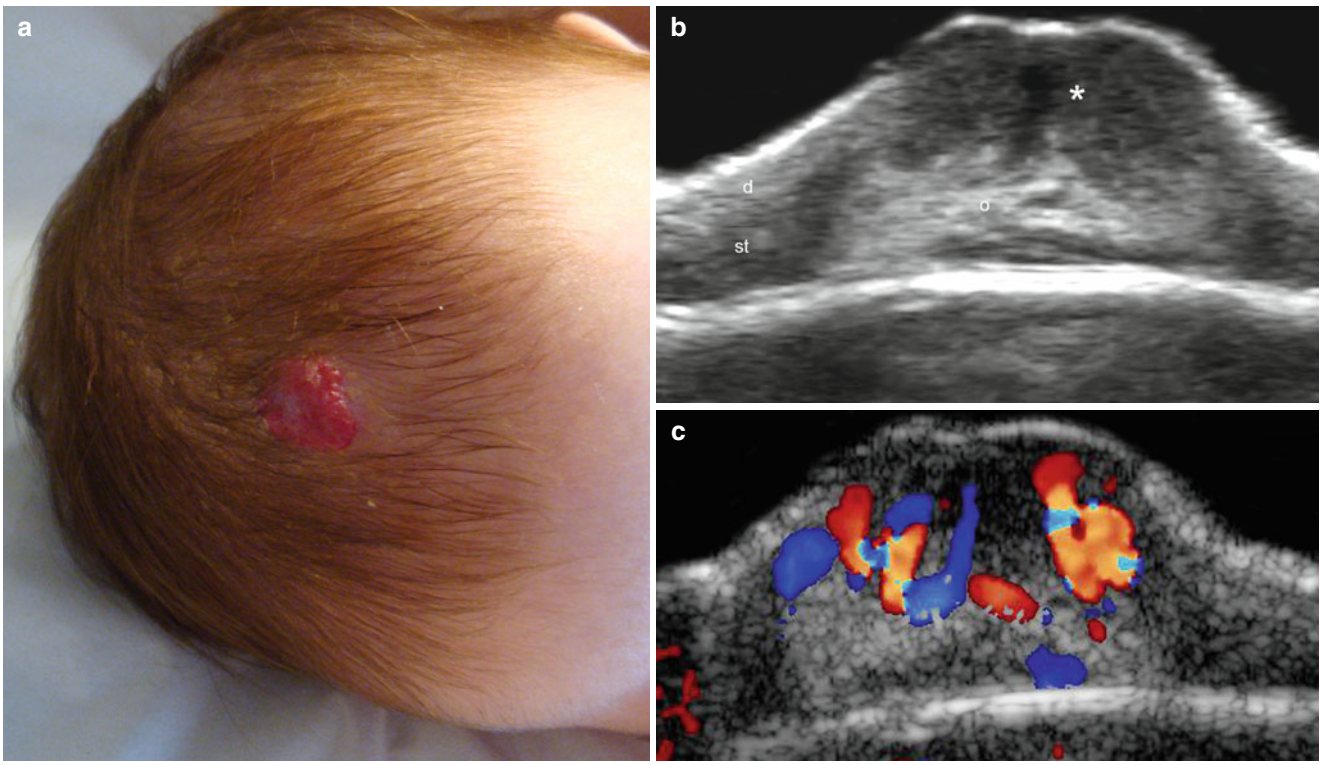

Fig. 19.14 (**a**–**c**) Hemangioma. (**a**) Clinical image shows a reddish swelling in the scalp. (**b**) Grey scale ultrasound image (transverse view) demonstrates an ill-defined heterogeneous structure that presents an upper hyperechoic area (*, mostly proliferative zone) and a lower hyperechoic area (o, mostly regression zone). (**c**) Color Doppler ultrasound image (transverse view) shows increased vascularity mostly in the upper region of the lesion. *Abbreviations*: *d* dermis, *st* subcutaneous tissue

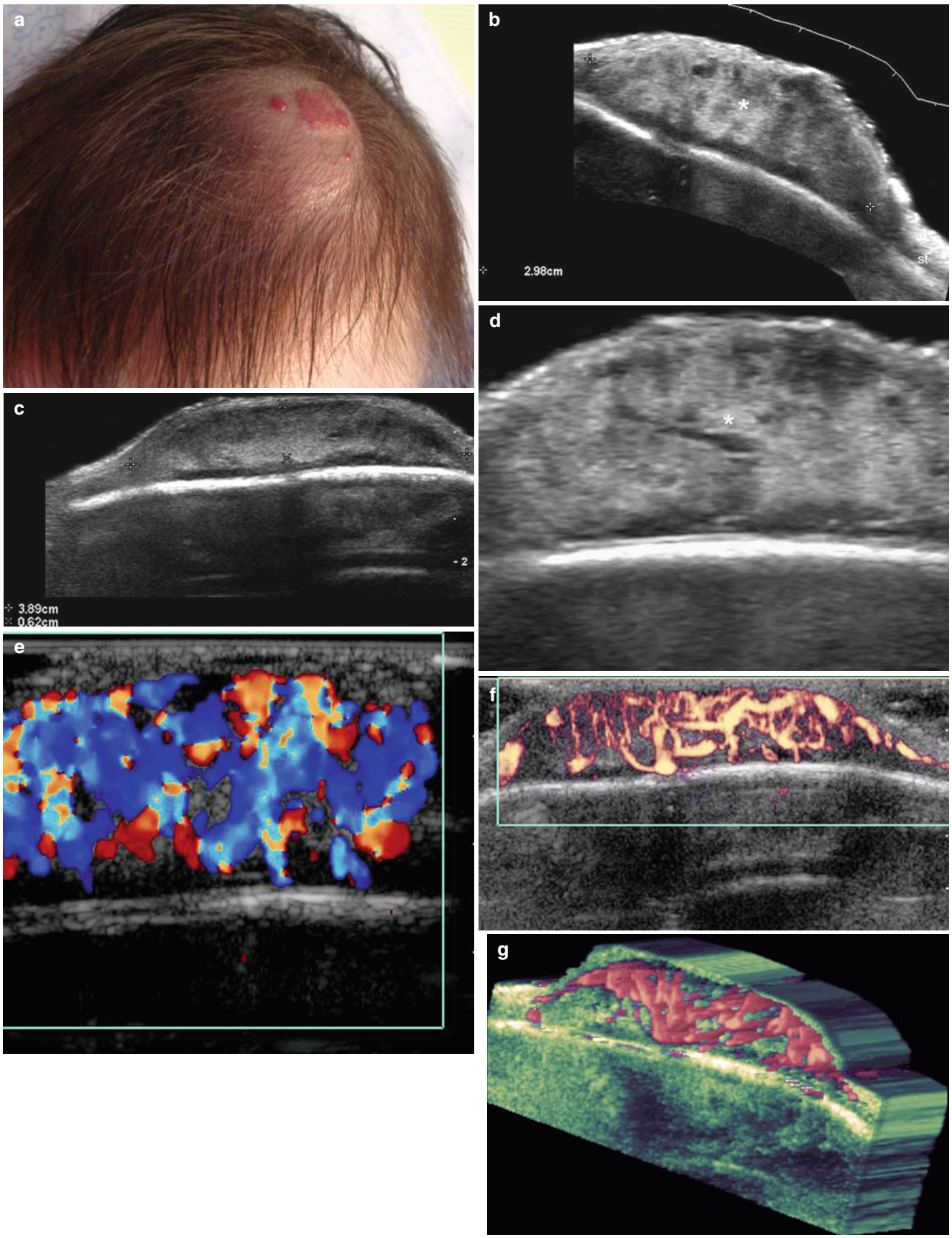

Fig. 19.15 (**a**–**g**) Hemangioma. (**a**) Clinical photograph shows a reddish lump. (**b**), (**c**, **d**) Grey scale ultrasound images (**b** longitudinal; **c** transverse and **d** zoomed transverse view) demonstrate a 3.98 cm (long) × 3.9 cm (transverse) × 0.62 (depth) ill-defined heterogeneous structure (*) mostly hyperechoic, located in the dermis and subcutaneous tissue. (**e**–**g**) Color and power Doppler ultrasound images (**e** color; **f** power; **g** 3D power angio reconstruction) show increased vascularity within the lesion

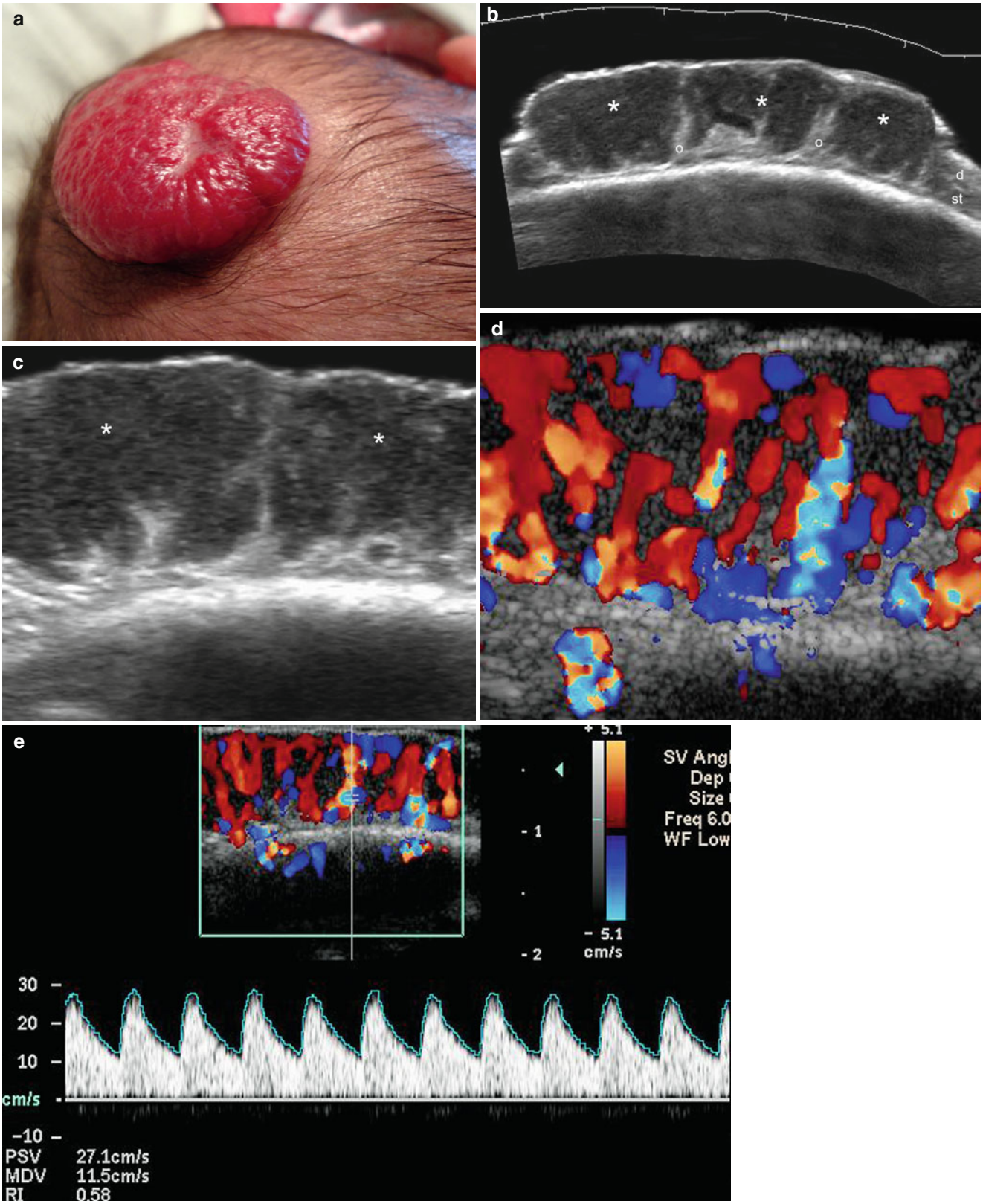

Fig. 19.16 (**a**–**g**) Hemangioma. (a) Clinical image shows a reddish lump in the left parietal region of the scalp. (**b**, **c**) Grey scale ultrasound images (**b**: extended field of transverse view; **c**: zoomed transverse view) demonstrate an ill-defined heterogeneous structure predominantly hypoechoic (*, mostly proliferative zone) and also presenting some hyperechoic deep areas (o, mostly regression zone). (**d**–**g**) Color Doppler ultrasound images (**d** zoomed image; **e** and **f** spectral curves; **g** 3D power angio reconstruction) show increased blood flow within the lesion. Notice that arterial (**e**) and venous (**f**) vessels are detected within the hemangioma. *Abbreviations*: *d* dermis, *st* subcutaneous tissue

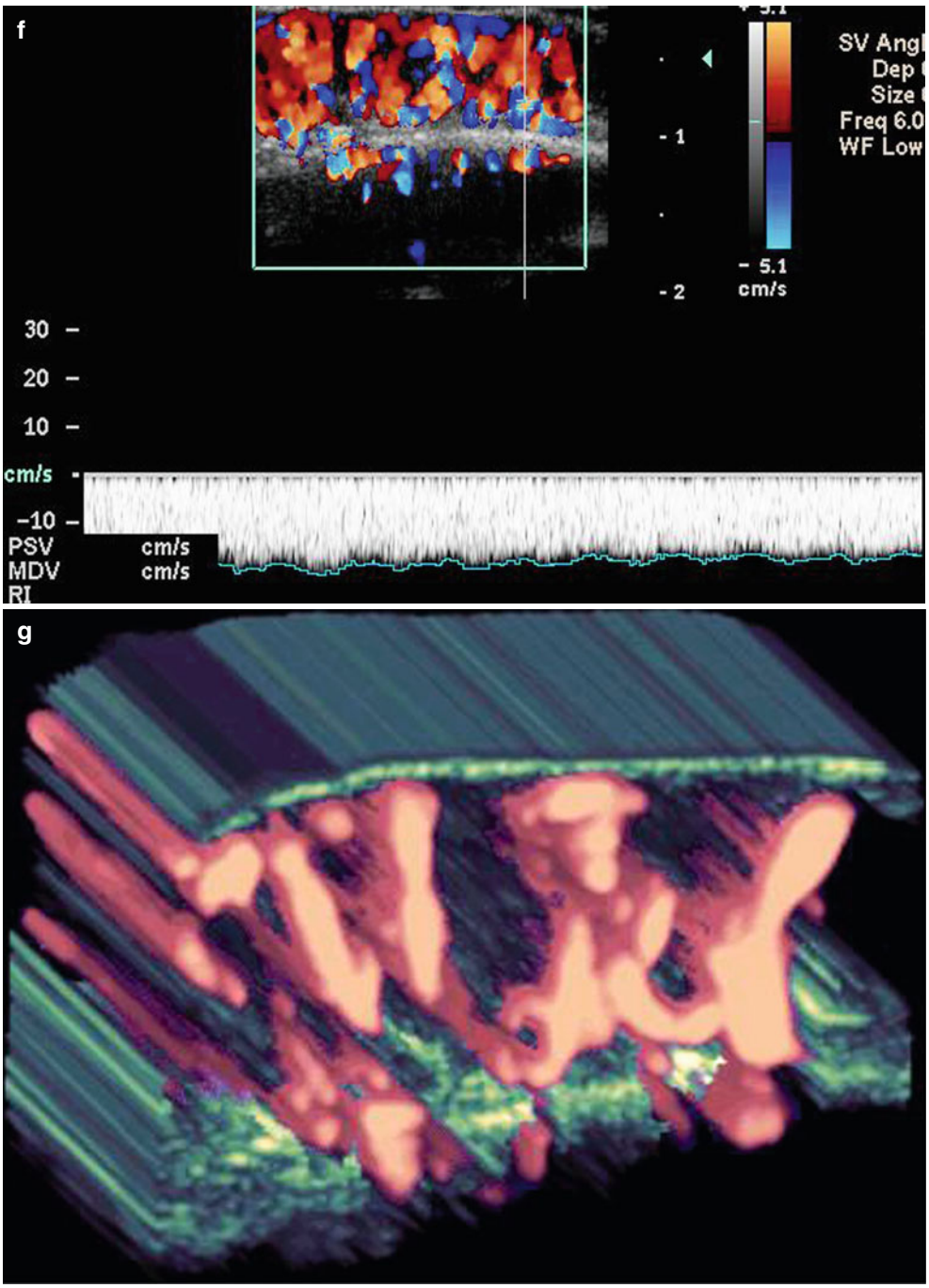

Fig. 19.16 (continued)

19.7.1.4 Scarring Alopecias

Scarring alopecias comprise a complex group of disorders with poorly defined origins that present with inflammation and scarring as common components [24, 25]. Sonography allows the characterizing of these entities on an anatomical basis and shows the different degrees of inflammation of the dermis and subcutaneous tissue. The latter findings appear on ultrasound as hypoechogenicity for the dermis, and hyperechogenicity for the subcutaneous tissue. Hypervascularity can be increased within the lesioned areas.

19.7.1.4.1 Acne Keloidalis Nuchae

Acne keloidalis nuchae (AKN) is a chronic scarring folliculitis seen mostly in young adult men who present with follicular papules and pustules coalescing occasionally into firm, shiny, smooth plaques and nodules on the nape of the neck. Acanthosis nigricans, a skin marker for the metabolic syndrome, obesity, curly hair, or wearing of a helmet has been associated with AKN. Additionally, AKN can present with some clinical similarities to acne inversa (hidradenitis suppurativa) [26]. Although AKN is infrequent, it has an important impact on the quality of life and may require aggressive treatment [26–29]. Sonography can show inflammation through all the cutaneous layers, hypoechoic connecting fistulous tracts, and enlargement of hair follicles [4] (Fig. 19.17).

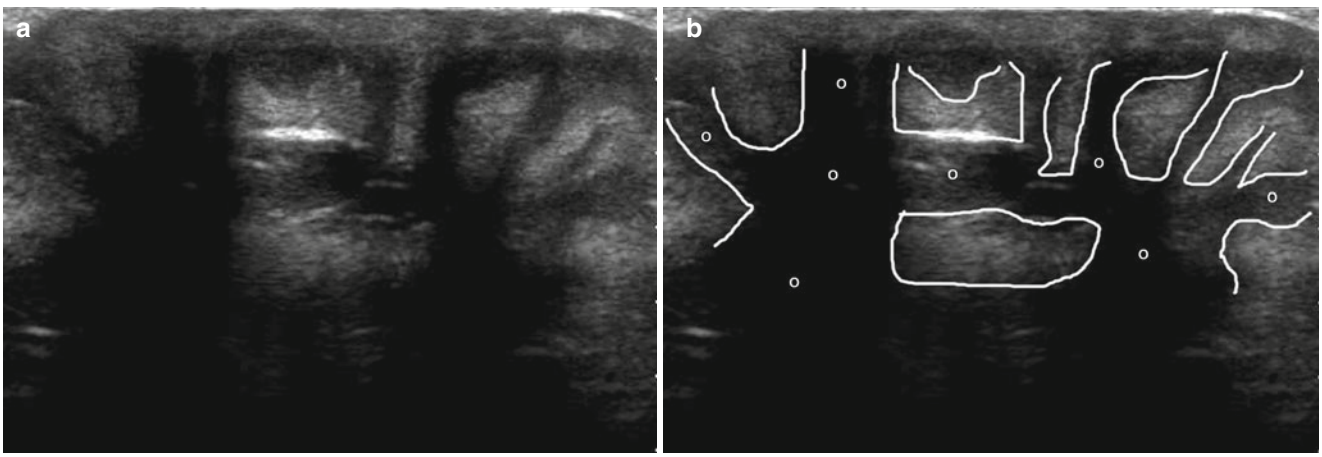

Fig. 19.17 (**a**, **b**) Acne keloidalis nuchae. (**a**, **b**) Grey scale ultrasound images (transverse view; **c** outlined) demonstrate multiple and connecting fistulous tracts (o) in the occipital region of the scalp

19.7.1.4.2 Perifolliculitis Capitis Abscedens et Suffodiens

Perifolliculitis capitis abscedens et suffodiens (PCAS) is a dissecting cellulitis or folliculitis of the scalp. PCAS is rare and presents as severe progressive inflammation with painful nodules and purulent drainage, with burrowing tracts connecting cutaneous fluid collections or abscesses and scarring as well as cicatricial alopecia [30, 31]. The etiology of PCAS is unknown but thought to follow episodes of follicular occlusion with reactive hyperkeratosis, secondary infection, and deep inflammation. PCAS may share its pathogenesis with acne conglobata and hidradenitis suppurativa, occurring as a triad [32]. Histologically, PCAS is a cicatricial neutrophilic alopecia with deep pustular inflammation at the reticular dermal or hypodermal levels. It starts with an episode of perifolliculitis that leaves deep abscesses and destroys the sebaceous glands that are then replaced by lymphoplasmocytic and giant cells granulomas [33]. Sonography of PCAS shows debris-filled fluid collections and/or abscesses with multiple connecting hypoechoic fistulous tracts that reach the hair bulb in the dermis and can cause follicular swelling. PCAS can affect large areas or the entire scalp, producing multiple areas of baldness [4] (Figs. 19.18 and 19.19).

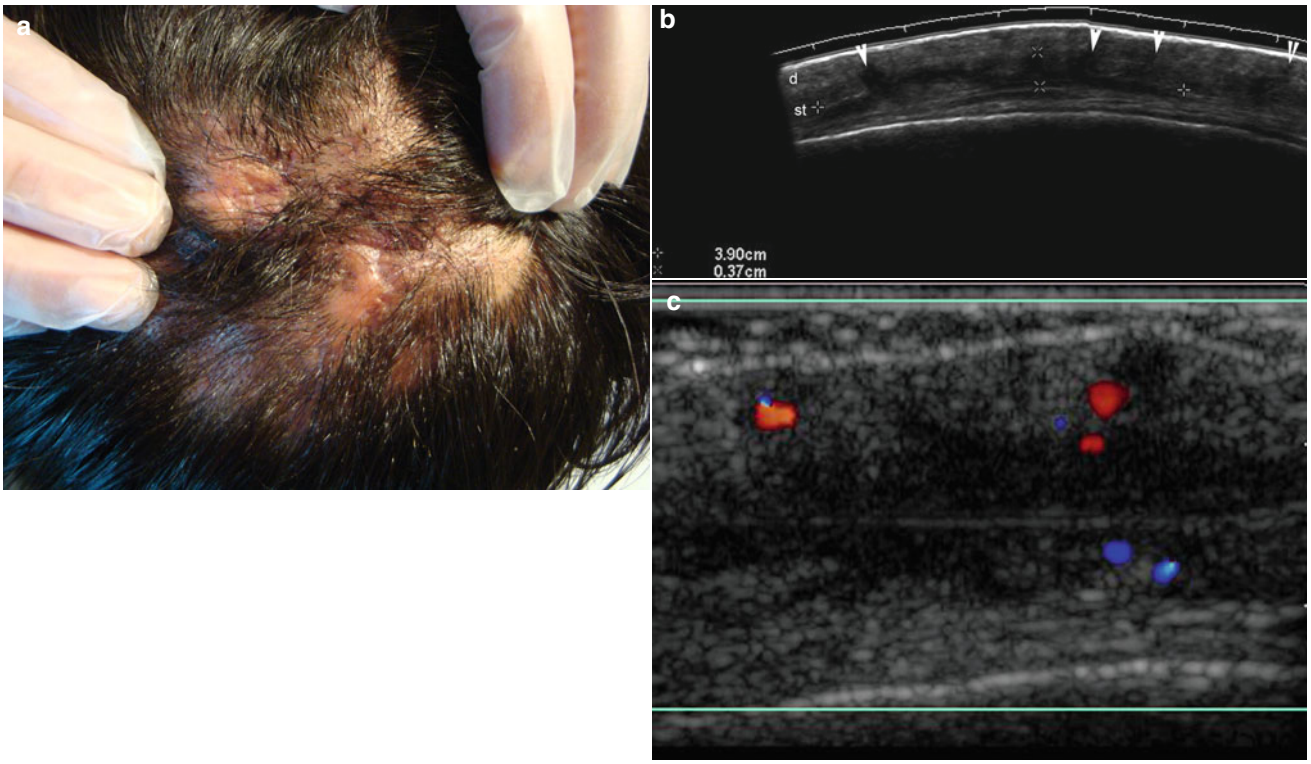

Fig. 19.18 (**a**–**c**) Perifolliculitis capitis abscedens et suffodiens. (**a**) Clinical image shows patchy alopecia. (**b**) Grey scale ultrasound image (transverse view) demonstrates a 3.9 cm (transverse) × 0.37 cm (depth) anechoic fluid collection (between markers) in the subcutaneous tissue with several connecting tracts (*arrowheads*) to the dermal region. (**c**) Color Doppler ultrasound image (transverse view) shows midly increased blood flow in the periphery of the fluid collection. *Abbreviations*: *d* dermis, *st* subcutaneous tissue

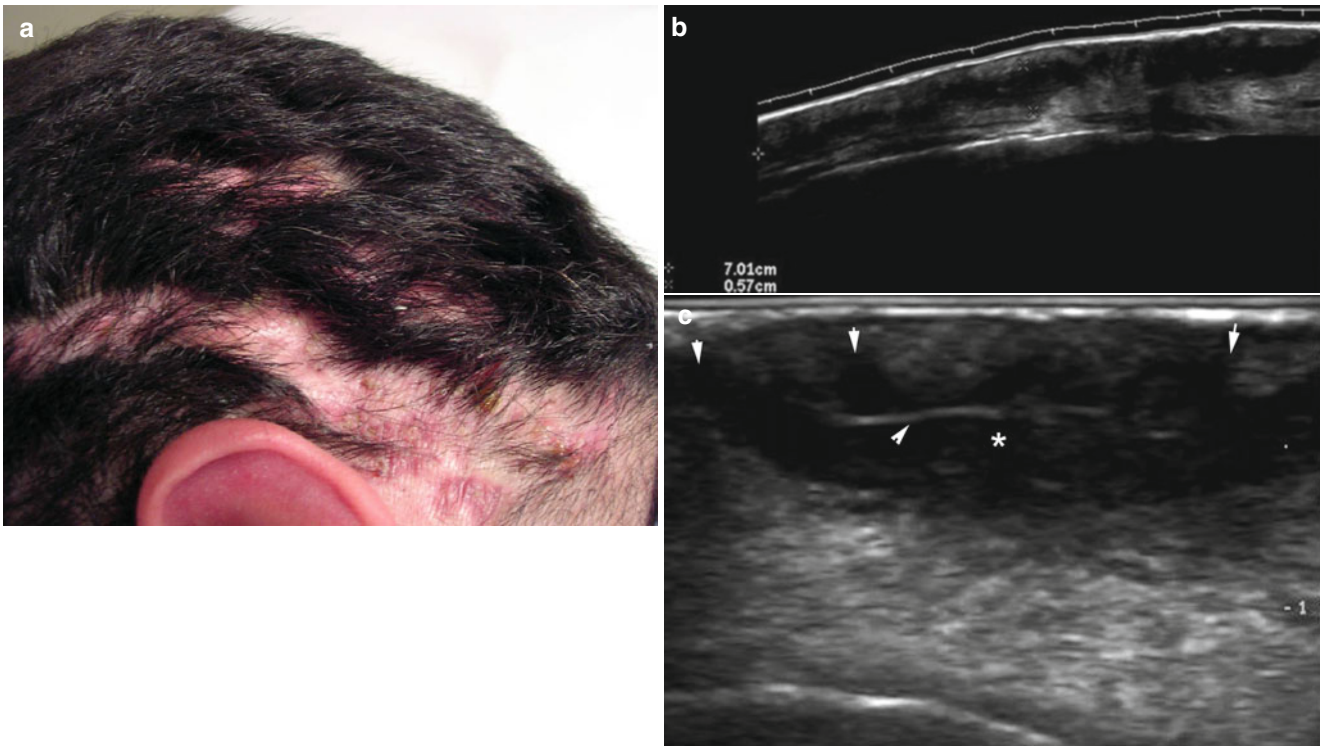

Fig. 19.19 (**a**–**c**) Perifolliculitis capitis abscedens et suffodiens. (**a**) Clinical photograph demonstrates patchy alopecia. (**b**) Grey scale ultrasound image (longitudinal view) shows a 7.0 cm (long) × 0.57 cm (depth) anechoic fluid collection (between markers) in the subcutaneous tissue. (**c**) Grey scale ultrasound image (zoomed transverse view) presents hyperechoic lines that correspond to hair tracts fragments (*arrowhead*) within the collection (*). Notice the connecting tracts (*arrows*) of the collection to dermis

19.7.1.4.3 Folliculitis Decalvans

Folliculitis decalvans (FD) is a chronic form of deep folliculitis that occurs on the scalp as patches of scarring alopecia at the expanding margins of which are the follicular pustules [34]. FD is a rare and recurrent purulent inflammation of the hair follicle in middle-aged adults that leads to scarring alopecia [35]. Both infection with *Staphylococcus aureus* and a deficient immune response by the host seem to be important for the development of this disfiguring disease [36]. The lesions typically occur in the vertex and occipital areas and consist of follicular pustules without external openings (ostia); there is also follicular tufting, surrounding diffuse or perifollicular erythema, and often hemorrhagic crusts and erosions can be seen. Early histology shows an inflammatory infiltrate of mainly neutrophils, followed by the additional recruitment of lymphocytes and plasma cells in more advanced stages [37]. Sonography shows inflammation of cutaneous layers, usually without fistulae, and thickening of hair follicles in the affected area. Hypoechoic scarring tissue and atrophy of the subcutaneous tissue can also be detected [4] (Fig. 19.20).

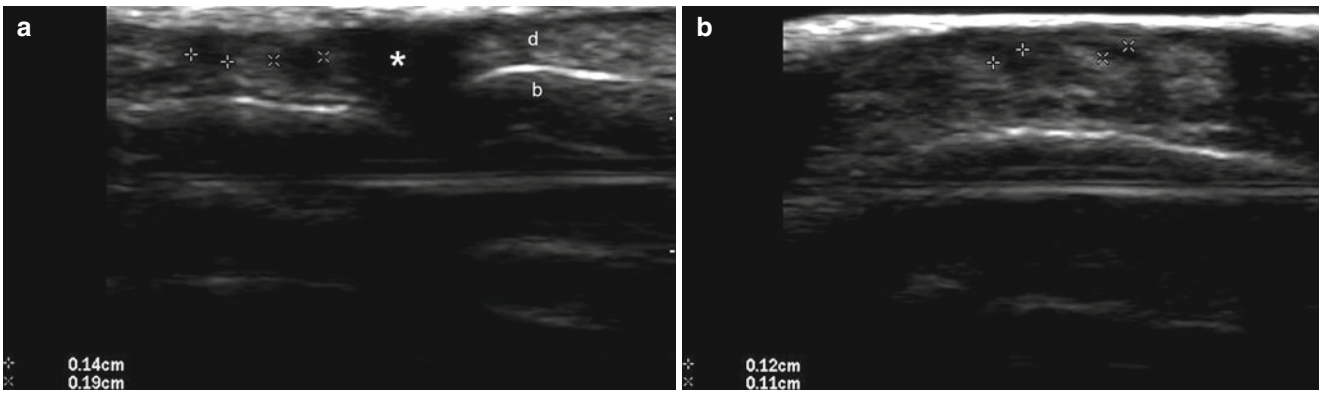

Fig. 19.20 (**a**, **b**) Folliculitis decalvans. (**a**, **b**) Grey scale ultrasound images (transverse views; parietal region) demonstrate thickening of the hair follicles (between markers) in the dermis and atrophy (post surgery and radiotherapy) of the subcutaneous tissue. There is a hypoechoic scar (*) in the site of a previous surgery. *Abbreviations*: *d* dermis, *b* bony margin of the skull

19.7.1.5 Pseudolymphoma

Pseudolymphoma, also called lymphocytoma cutis and cutaneous lymphoid hyperplasia implies a proliferation of lymphocytes in response to a foreign antigen or unknown stimuli [38]. Cutaneous pseudolymphomas comprise a heterogeneous group of lymphoproliferative disorders with dermal infiltrates of benign reactive T-cells or B-cells that tend to regress spontaneously over time [39]. Pseudolymphomas can simulate cutaneous lymphomas at both clinical and histological levels, developing as reactions to antigenic stimuli as varied as arthropod bites, vaccinations, tattoos, infections, or drugs; pseudolymphoma can also be idiopathic [40–44]. Sonography shows a focal and sometimes fusiform- or oval-shaped thickening of the dermis; this focal region presents hypoechogenicity but can become heterogeneous. Additionally, there is usually increased blood flow within the lesion and the periphery [4] (Fig. 19.21).

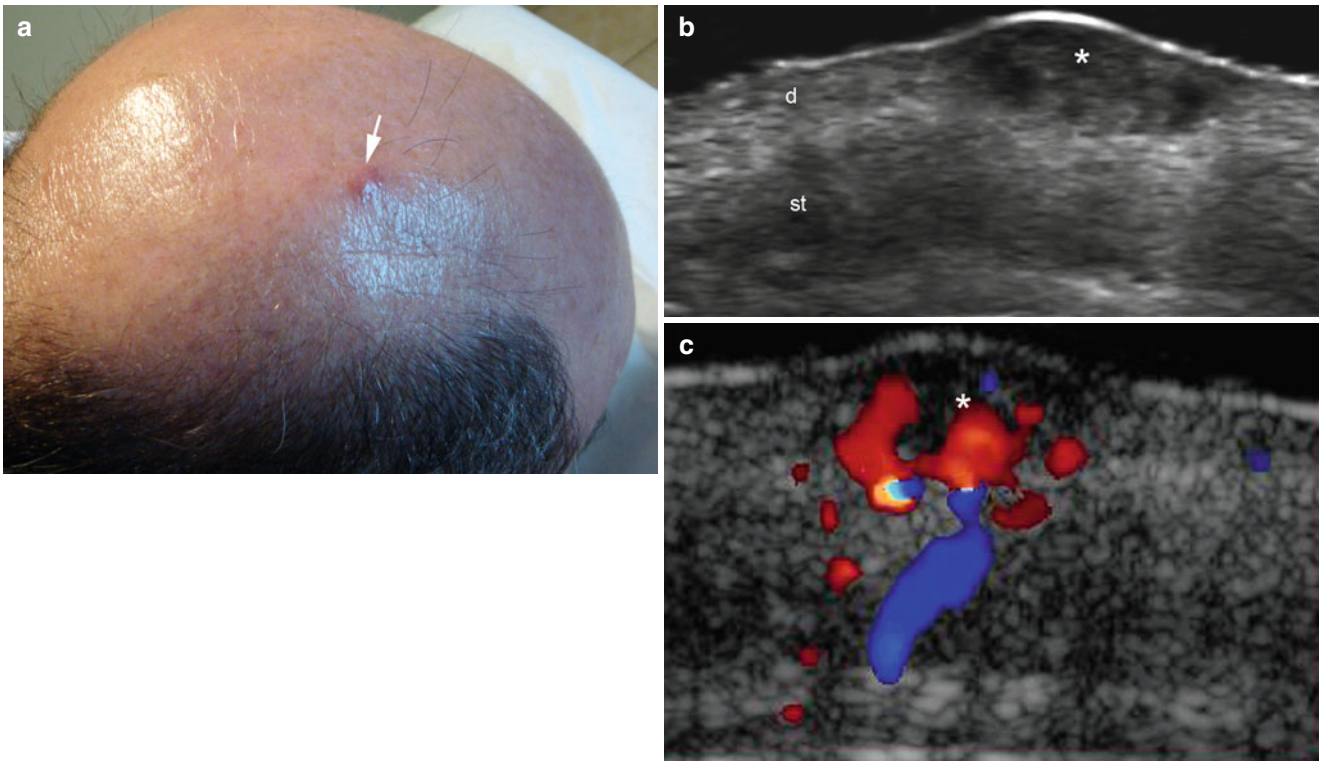

Fig. 19.21 (**a**–**c**) Pseudolymphoma. (**a**) Clinical image demonstrates a reddish lump (*arrow*) in the scalp (right parietal region). (**b**) Grey scale ultrasound image (transverse view) demonstrates an oval-shaped hypoechoic and heterogeneous structure (*) that affects the dermis. (**c**) Color Doppler ultrasound image (transverse view) shows increased blood flow within the lesion (*) and the surrounding tissues *Abbreviations*: *d* dermis, *st* subcutaneous tissue

19.7.2 Malignant Conditions

19.7.2.1 Skin Cancer

Malignant tumors occurring in the scalp are not common and when asymptomatic or small in size, may be covered by hair and neglected by the patient, leading to a potential risk of delay in detection and resulting in poorer outcomes [45]. Thus, cutaneous cancers of the scalp represent approximately 2 % of all skin cancers, with basal cell carcinoma being the most frequent in women and squamous cell carcinoma in men [46, 47]. Risk factors for developing skin cancer of the scalp include actinic damage, prior treatment with ionizing radiation, immunosuppresion, chronic scarring, and coexisting genodermatosis [48]. Alopecia favors the development of skin cancer from the direct exposure of the skin to solar radiation in men [48]. Features associated with recurrences include prior anticancer treatment, immunosuppression, and tumors of a large size; in fact, scalp cancer may already extend microscopically for a significant distance away from the primary site at the time of diagnosis, because the subgaleal plane offers little resistance to tumor spread. Furthermore, if the tumor penetrates the periosteum, it can spread laterally for even greater distances [46, 49]. Sonography of scalp cancer shows hypoechoic solid lesions of generally increased vascularity [50], and in basal cell carcinoma, hyperechoic spots can be detected within the tumor [51] (Figs. 19.22, 19.23, 19.24, 19.25, and 19.26).

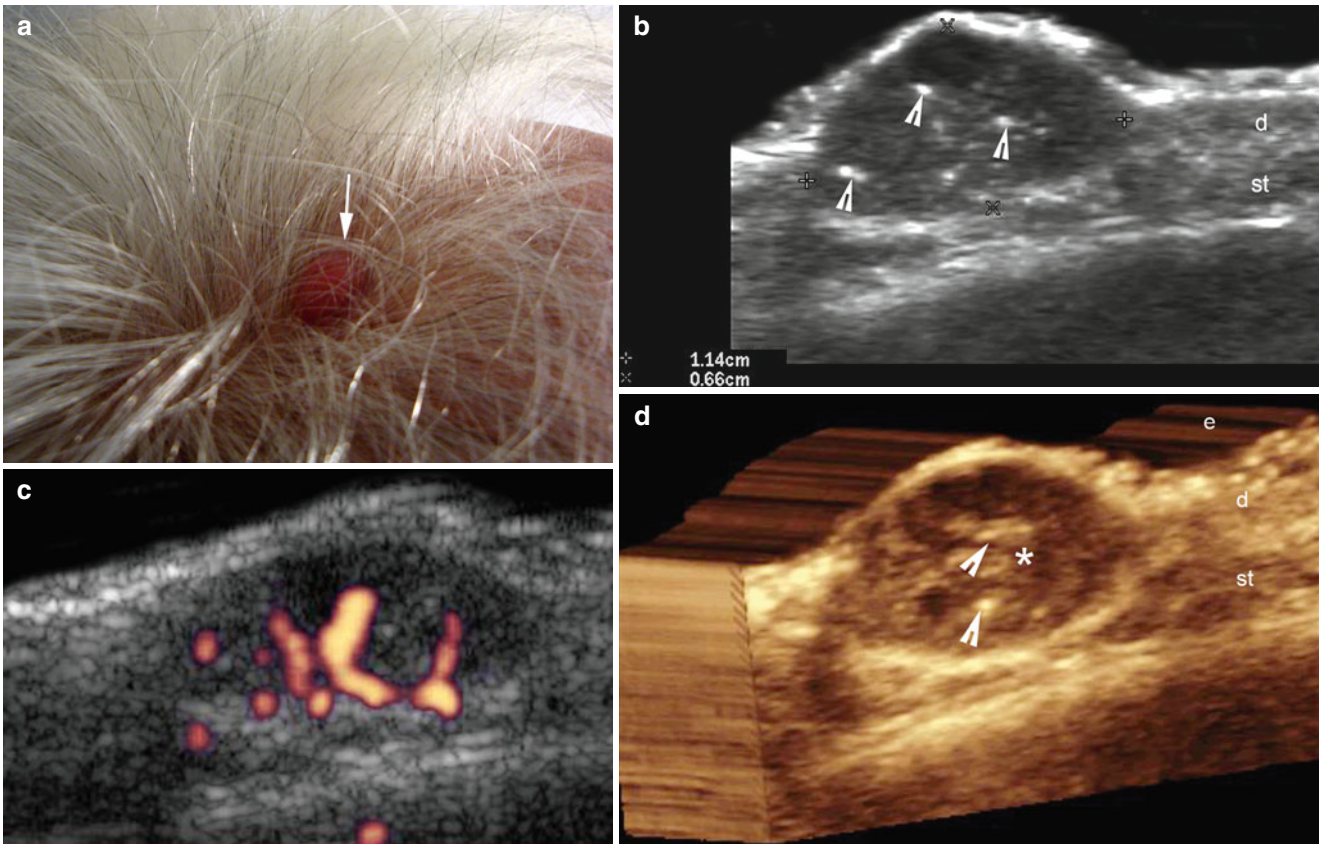

Fig. 19.22 (**a**–**d**) Basal cell carcinoma. (**a**) Clinical photograph demonstrates a reddish lump (*arrow*) in the scalp. (**b**) Grey scale ultrasound image (transverse view; right frontal region of the scalp) shows 1.14 cm (transverse) × 0.66 cm (depth) well-defined hypoechoic and heterogeneous structure (between markers) that involves the dermis and subcutaneous tissue. Notice the hyperechoic spots (*arrowheads*) within the lesion. (**c**) Power Doppler ultrasound image (longitudinal view) demonstrates increased vascularity within the lesional area. (**d**) 3D reconstruction (transverse view) highlights the tumor (*) and its hyperechoic spots (*arrowheads*). *Abbreviations*: *e* epidermis, *d* dermis, *st* subcutaneous tissue

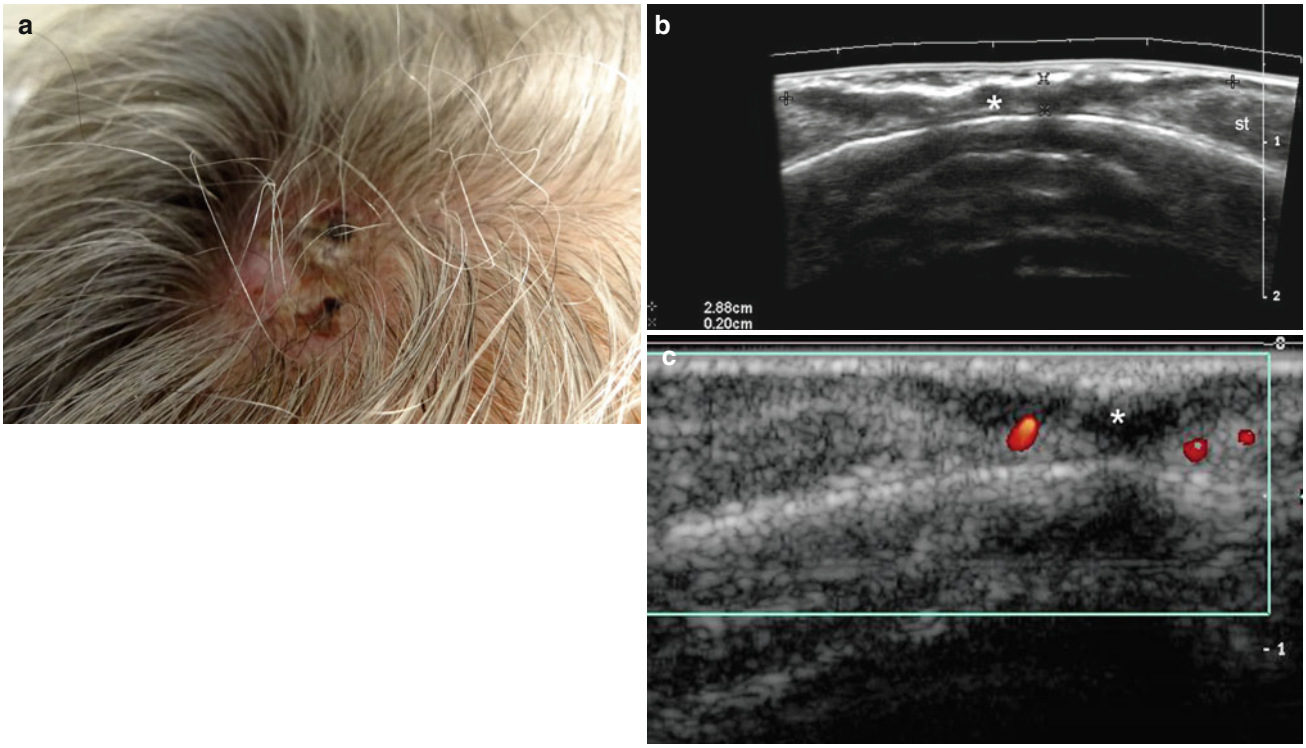

Fig. 19.23 (**a**–**c**) Basal cell carcinoma. (**a**) Clinical image shows erythematous, pigmented, crusty, and scaly lesion in the right frontal region of the scalp. (**b**) Grey scale ultrasound image (transverse view) demonstrates a 2.88 cm (transverse) × 0.37 cm (depth) hypoechoic structure (*, between markers) that affects the epidermis, dermis, and subcutaneous tissue. Notice the hyperechoic epidermal thickening in the lesional region. (**c**) Color Doppler ultrasound image (longitudinal view) shows mildly increased vascularity in the periphery of the lesion

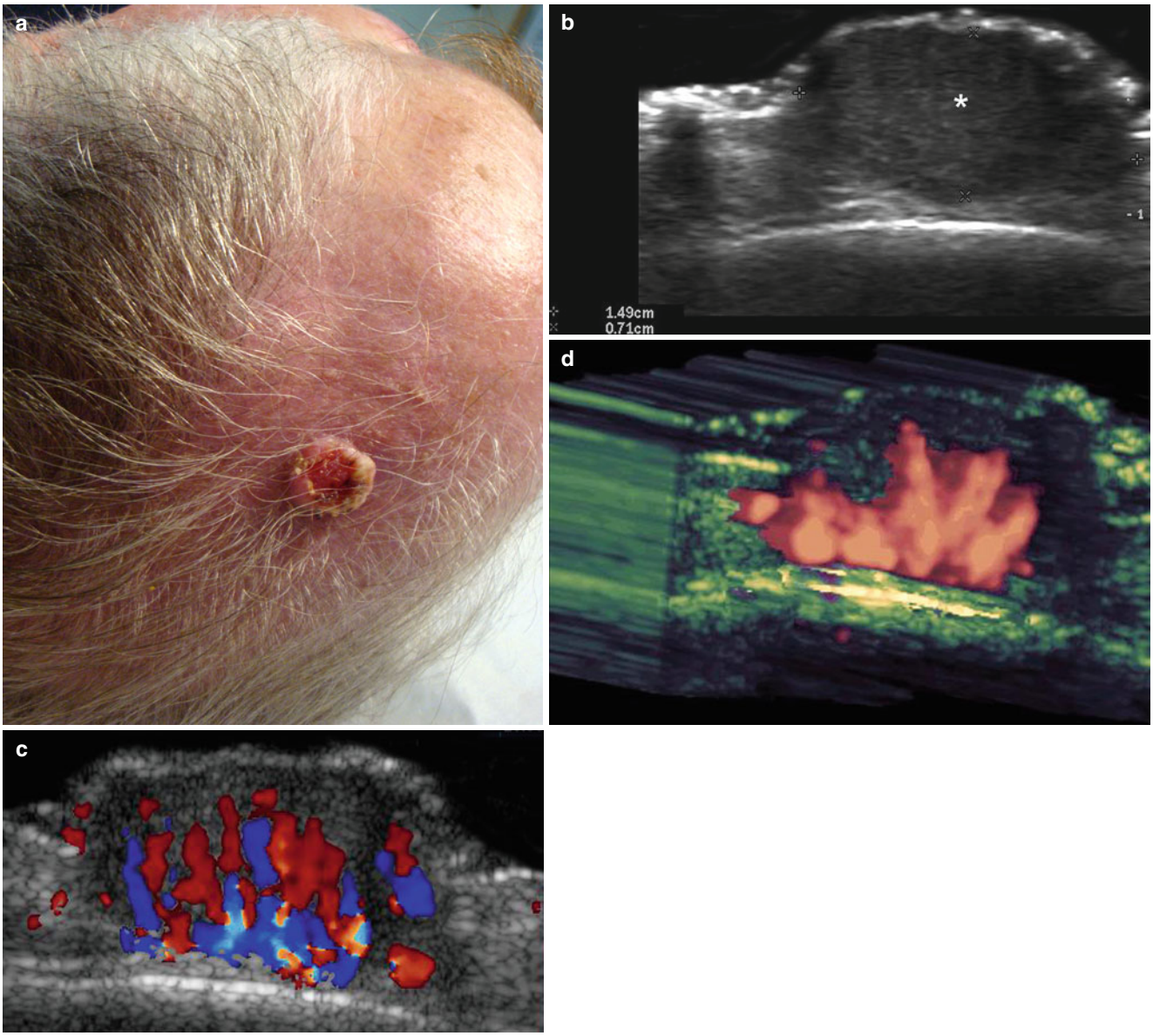

Fig. 19.24 (**a**–**d**) Squamous cell carcinoma. (**a**) Clinical image demonstrates erythematous and ulcerated lump in the left parietal region of the scalp. (**b**) Grey scale ultrasound image (transverse view) shows a 1.49 cm (transverse) × 0.71 (depth) well-defined hypoechoic solid mass (*) that affects the dermis and subcutaneous tissue. (**c**) Color Doppler ultrasound image (longitudinal view) shows strong vascularity within the mass. (**d**) 3D power angio reconstruction highlights the blood flow of the mass

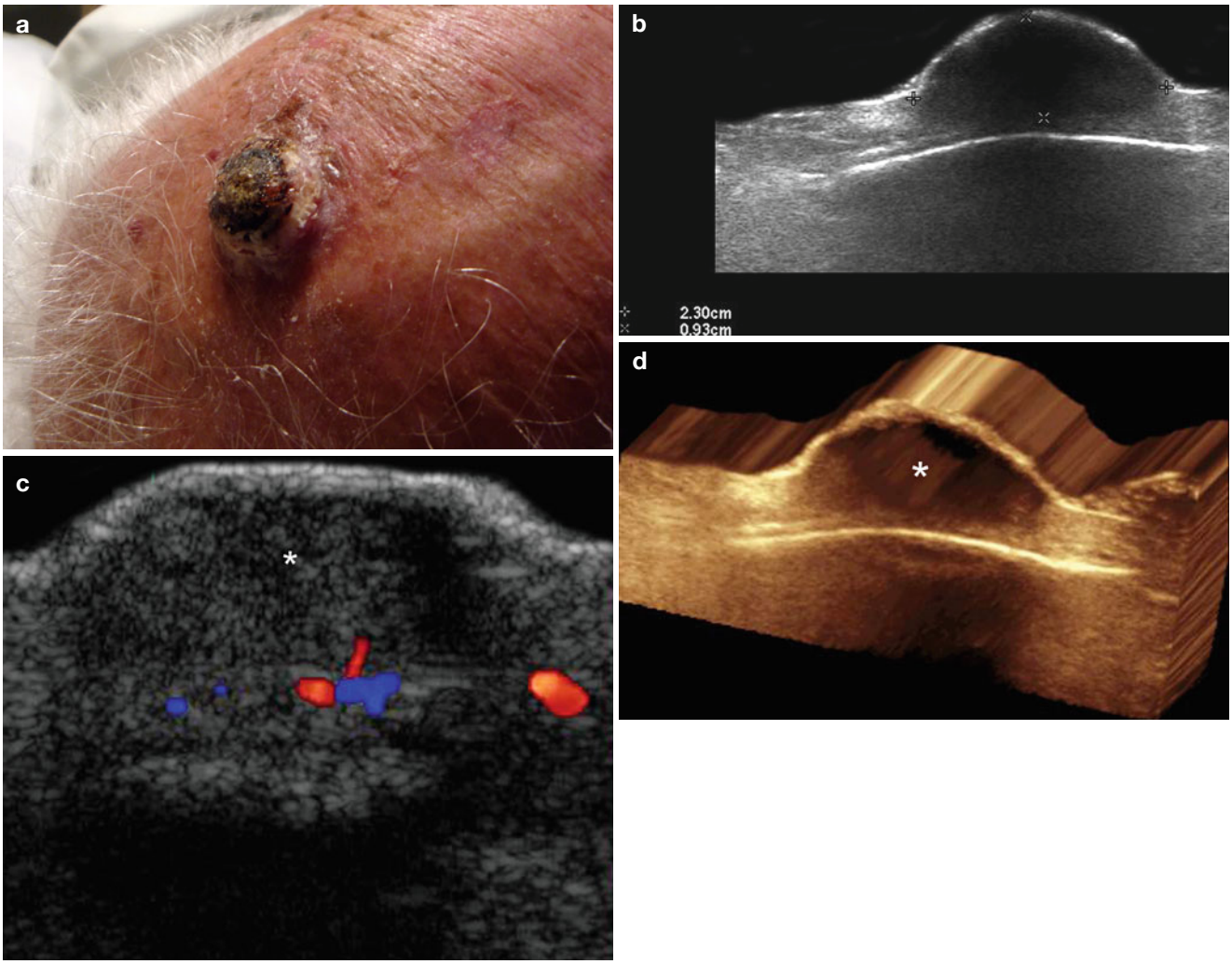

Fig. 19.25 (**a**–**d**) Squamous cell carcinoma. (**a**) Clinical photograph demonstrates a pigmented outgrowth in the left parietal region of the scalp. (**b**) Grey scale ultrasound image (transverse view) shows a 2.3 cm (transverse) × 0.93 cm (depth) hypoechoic mass (*, between markers) that involves the dermis and subcutaneous tissue. (**c**) Color Doppler ultrasound image (longitudinal view) demonstrates slightly increased blood flow in the periphery of the mass. (**d**) 3D reconstruction of the mass (*)

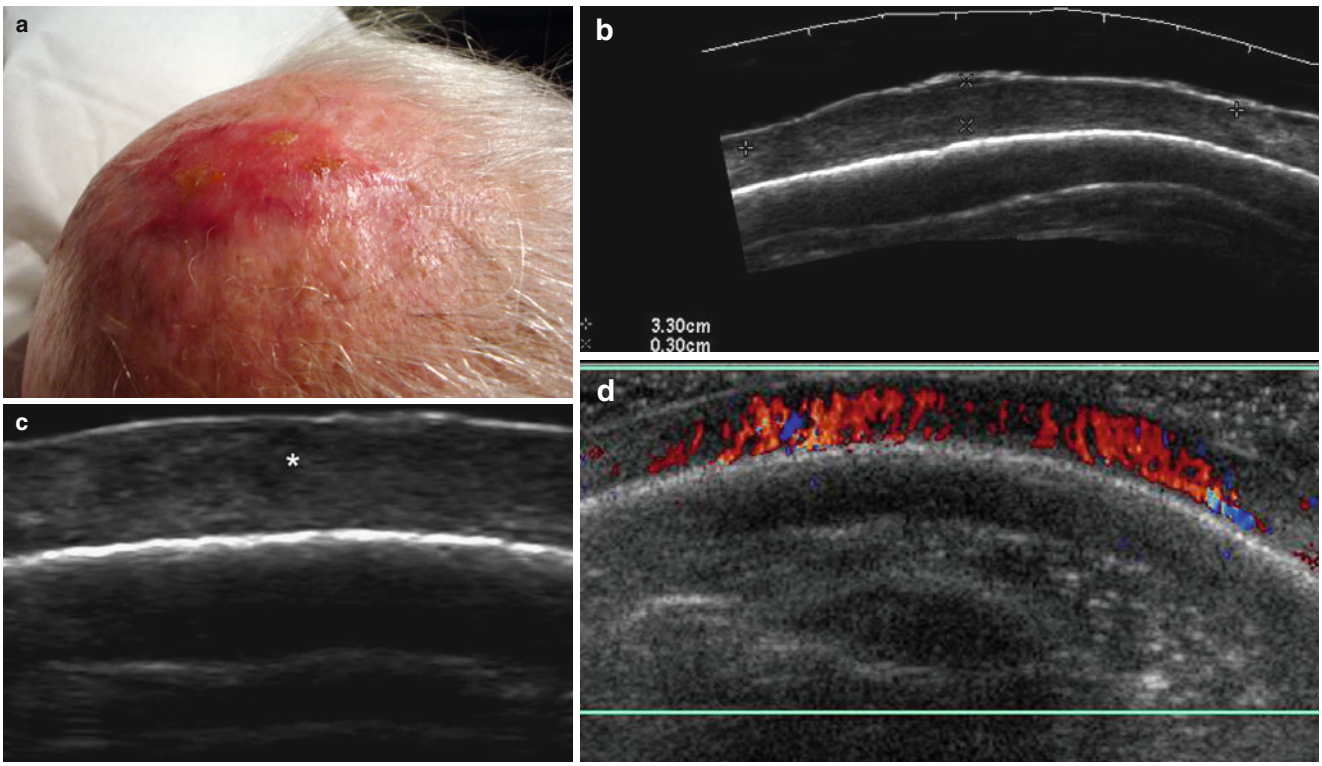

Fig. 19.26 (**a**–**d**) Squamous cell carcinoma. (**a**) Clinical photograph shows erythematous plaque-like swelling in the left parietal region of the scalp. (**b**, **c**) Grey scale ultrasound images (**b** extended transverse field of view; **c** zoomed longitudinal view) demonstrate a 3.3 cm (transverse) × 0.3 cm (depth) hypoechoic and heterogeneous thickening (*, between markers) of the dermis and subcutaneous tissue. (**d**) Color Doppler ultrasound image (longitudinal view) shows strong vascularity in the lesion area

Folliculotropic mycosis fungoides (FMF), a low-grade lymphoproliferative disorder, is a rare variant of cutaneous T-cell lymphoma where the neoplastic T lymphocytes display tropism for the follicular epithelium [52]. It presents clinically with patches, plaques, acneiform lesions (comedo-like and/or epidermal cysts), palpable tumors, and/or erythroderma. The most common site of involvement of the folliculotropic form of mycosis fungoides is the head and neck (80 %), with alopecia as a frequent sequel to head involvement. Histologically, FMF shows selective infiltration of the follicular epithelium by atypical lymphocytes and mucinous degeneration of the follicular epithelium in 60 % of cases [53, 54]. Sonography will show general thickening of the skin, decreased echogenicity of the upper dermis, thickening of the hair follicles, and hyperechoic deposits surrounding large hypoechoic hair follicles in the scalp or any FMF-affected area of the body [4] (Fig. 19.27).

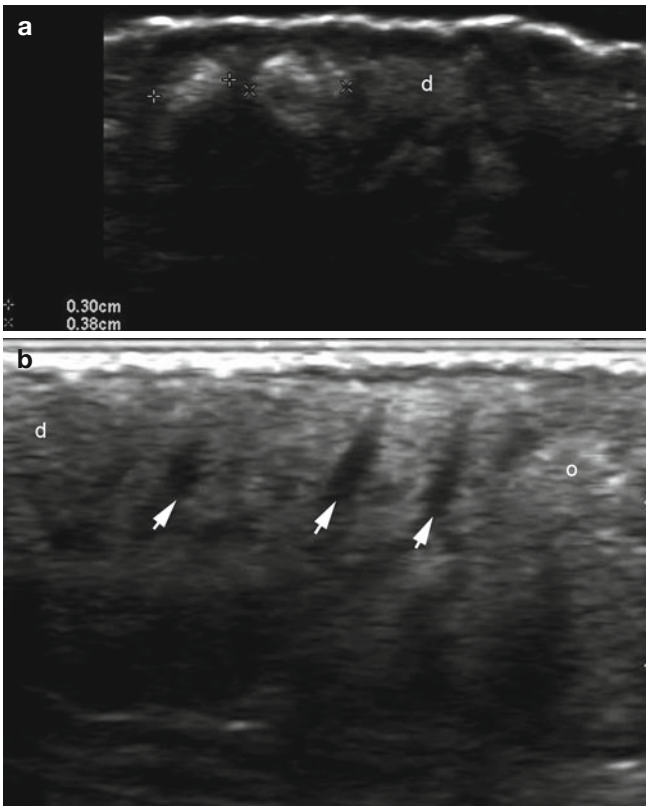

Fig. 19.27 (**a**, **b**) Folliculotropic mycosis fungoides. (**a**, **b**) Grey scale ultrasound images (occipital region of the scalp (**a** transverse; **b** longitudinal view). (**a**) Ultrasound image demonstrates hyperechoic deposits (between markers) surrounding the dermal hair follicles. (**b**) Ultrasound image shows thickening of the dermal hair follicles (*arrows*) and some hyperechoic deposits (o). *Abbreviation*: *d* dermis

References

1. Miyakoshi K, Tanaka M, Matsumoto T, Hattori Y, Minegishi K, Ishimoto H, et al. Occipital scalp hemangioma: prenatal sonographic and magnetic resonance images. J Obstet Gynaecol Res. 2008;34:666–9.
2. Wolfram LJ. Human hair: a unique physicochemical composite. J Am Acad Dermatol. 2003;48:S106–14.
3. Thibaut S, De Becker E, Caisey L, Baras D, Karatas S, Jammayrac O, et al. Human eyelash characterization. Br J Dermatol. 2010;162:304–10.
4. Wortsman X, Wortsman J, Matsuoka L, Saavedra T, Mardones F, Saavedra D, et al. Sonography in pathologies of scalp and hair. Br J Radiol. 2012;85(1013):647–55.
5. Wortsman X, Wortsman J. Clinical usefulness of variable-frequency ultrasound in localized lesions of the skin. J Am Acad Dermatol. 2010;62(2):247–56.
6. Seery GE. Surgical anatomy of the scalp. Dermatol Surg. 2002;28:581–7.
7. Al-Nuaimi Y, Baier G, Watson RE, Chuong CM, Paus R. The cycling hair follicle as an ideal systems biology research model. Exp Dermatol. 2010;19:707–13.
8. Yagyu K, Hayashi K, Chang SC. Orientation of multi-hair follicles in nonbald men: perpendicular versus parallel. Dermatol Surg. 2006;32:651–60.
9. Mattle E, Weiger M, Schmidig D, Boesiger P, Fey M. MRI of human hair. MAGMA. 2009;22:181–6.
10. Wortsman X, Wortsman J, Soto R, et al. Benign tumors and pseudotumors of the nail: a novel application of sonography. J Ultrasound Med. 2010;29:803–16.
11. Sau P, Graham JH, Helwig EB, Sau P, Graham JH, Helwig EB. Proliferating epithelial cysts. Clinicopathological analysis of 96 cases. J Cutan Pathol. 1995;22:394–406.
12. Satyaprakash AK, Sheehan DJ, Sangüeza OP. Proliferating trichilemmal tumors: a review of the literature. Dermatol Surg. 2007;33:1102–8.
13. Anolik R, Firoz B, Walters RF, Meehan SA, Tsou HC, Whitlow M, et al. Proliferating trichilemmal cyst with focal calcification. Dermatol Online J. 2008;14:25.
14. Agarwal RP, Handler SD, Matthews MR, Carpentieri D. Pilomatrixoma of the head and neck in children. Otolaryngol Head Neck Surg. 2001;125:510–5.
15. Roche NA, Monstrey SJ, Matton GE. Pilomatricoma in children: common but often misdiagnosed. Acta Chir Belg. 2010;110:250–4.
16. Cecen E, Ozguven AA, Uysal KM, Gunes D, Ozer E, Olgun N, et al. Pilomatricoma in children: a frequently misdiagnosed superficial tumor. Pediatr Hematol Oncol. 2008;25:522–7.
17. Choo HJ, Lee SJ, Lee YH, Lee JH, Oh M, Kim MH, et al. Pilomatricomas: the diagnostic value of ultrasound. Skeletal Radiol. 2010;39:243–50.
18. Hwang JY, Lee SW, Lee SM. The common ultrasonographic features of pilomatricoma. J Ultrasound Med. 2005;24:1397–402.
19. Peer S. The place of sonography in the diagnostic work-up of haemangiomas and vascular malformations. Handchir Mikrochir Plast Chir. 2009;41:70–7.
20. Giovagnorio F, Andreoli C, De Cicco ML. Color Doppler sonography of focal lesions of the skin and subcutaneous tissue. J Ultrasound Med. 1999;18:89–93.
21. Wortsman X. Common applications of dermatologic sonography. J Ultrasound Med. 2012;31(1):97–111.
22. Verity DH, Rose GE, Restori M. The effect of intralesional steroid injections on the volume and blood flow in periocular capillary haemangiomas. Orbit. 2008;27:41–7.

23. Sans V, de la Roque ED, Berge J, et al. Propranolol for severe infantile hemangiomas: follow-up report. Pediatrics. 2009;124:423–31.
24. Al-Zaid T, Vanderweil S, Zembowicz A, Lyle S. Sebaceous gland loss and inflammation in scarring alopecia: a potential role in pathogenesis. J Am Acad Dermatol. 2011;65(3):597–603.
25. Stefanato CM. Histopathology of alopecia: a clinicopathological approach to diagnosis. Histopathology. 2010;56:24–38.
26. Verma SB, Wollina U. Acne keloidalis nuchae: another cutaneous symptom of metabolic syndrome, truncal obesity, and impending/overt diabetes mellitus? Am J Clin Dermatol. 2010;11(6):433–6.
27. Sterling JB, Sina B, Gaspari A, Deng A. Acne keloidalis: a novel presentation for tinea capitis. J Am Acad Dermatol. 2007;56:699–701.
28. Bajaj V, Langtry JA. Surgical excision of acne keloidalis nuchae with secondary intention healing. Clin Exp Dermatol. 2008;33:53–5.
29. Gloster Jr HM. The surgical management of extensive cases of acne keloidalis nuchae. Arch Dermatol. 2000;136:1376–9.
30. Brănişteanu DE, Molodoi A, Ciobanu D, et al. The importance of histopathologic aspects in the diagnosis of dissecting cellulitis of the scalp. Rom J Morphol Embryol. 2009;50:719–24.
31. Mihić LL, Tomas D, Situm M, Krolo I, Sebetić K, Sjerobabski-Masnec I, et al. Perifolliculitis capitis abscedens et suffodiens in a Caucasian: diagnostic and therapeutic challenge. Acta Dermatovenerol Croat. 2011;19(2):98–102.
32. Ljubojevic S, Pasic A, Lipozencic J, Skerlev M. Perifolliculitis capitis abscedens et suffodiens. J Eur Acad Dermatol Venereol. 2005;19:719–21.
33. Williams CN, Cohen M, Ronan SG, Lewandowski CA. Dissecting cellulitis of the scalp. Plast Reconstr Surg. 1986;77:378–82.
34. Castaño-Suárez E, Romero-Maté A, Arias-Palomo D, Borbujo J. Photodynamic therapy for the treatment of folliculitis decalvans. Photodermatol Photoimmunol Photomed. 2012;28(2):102–4.
35. Otberg N, Kang H, Alzolibani AA, Shapiro J. Folliculitis decalvans. Dermatol Ther. 2008;21:238–44.
36. Gemmeke A, Wollina U. Folliculitis decalvans of the scalp: response to triple therapy with isotretinoin, clindamycin, and prednisolone. Acta Dermatovenerol Alp Panonica Adriat. 2006;15:184–6.
37. Chiarini C, Torchia D, Bianchi B, Volpi W, Caproni M, Fabbri P. Immunopathogenesis of folliculitis decalvans: clues in early lesions. Am J Clin Pathol. 2008;130:526–34.
38. Nnebe NV, Woon C, Haines S, Dayton V, Weigel BJ. Cutaneous pseudolymphoma: an unusual presentation of a scalp mass. Pediatr Blood Cancer. 2009;52(2):283–5.
39. Bergman R. Pseudolymphoma and cutaneous lymphoma: facts and controversies. Clin Dermatol. 2010;28:568–74.
40. Bachelez H. The uncertain status of cutaneous pseudolymphoma. Actas Dermosifiliogr. 2009;100:33–7.
41. Cerroni L, Borroni RG, Massone C, Chott A, Kerl H. Cutaneous B-cell pseudolymphoma at the site of vaccination. Am J Dermatopathol. 2007;29:538–42.
42. Gutermuth J, Hein R, Fend F, Ring J, Jakob T. Cutaneous pseudolymphoma arising after tattoo placement. J Eur Acad Dermatol Venereol. 2007;21:566–7.
43. Colli C, Leinweber B, Müllegger R, Chott A, Kerl H, Cerroni L. Borrelia burgdorferi-associated lymphocytoma cutis: clinicopathologic, immunophenotypic, and molecular study of 106 cases. J Cutan Pathol. 2004;31:232–40.
44. Ploysangam T, Breneman DL, Mutasim DF. Cutaneous pseudolymphomas. J Am Acad Dermatol. 1998;38:877–95.
45. Greco M, Vitagliano T, Fiorillo MA, Atzeni M, Corona A, Ribuffo D. Rare malignant tumors of the scalp: a report of four cases, their treatment and a review of the literature. Eur Rev Med Pharmacol Sci. 2010;14(11):993–7.
46. Lang Jr PG, Braun MA, Kwatra R. Aggressive squamous carcinomas of the scalp. Dermatol Surg. 2006;32:1163–70.
47. Katz TM, Silapunt S, Goldberg LH, Jih MH, Kimyai-Asadi A. Analysis of 197 female scalp tumors treated with mohs micrographic surgery. J Am Acad Dermatol. 2005;52:291–4.
48. Neubauer KE, Goldstein GD, Plumb SJ. Squamous cell carcinoma of the scalp in organ transplant recipients: exploring mechanisms for recurrence and treatment guidelines. Dermatol Surg. 2010;36:185–93.
49. Leibovitch I, Huilgol SC, Richards S, Paver R, Selva D. Scalp tumors treated with mohs micrographic surgery: clinical features and surgical outcome. Dermatol Surg. 2006;32:1369–74.
50. Bobadilla F, Wortsman X, Muñoz C, Segovia L, Espinoza M, Jemec GBE. Pre-surgical high resolution ultrasound of facial basal cell carcinoma: correlation with histology. Cancer Imaging. 2008;22:163–72.
51. Uhara H, Hayashi K, Koga H, Saida T. Multiple hypersonographic spots in basal cell carcinoma. Dermatol Surg. 2007;33:1215–9.
52. Muniesa C, Estrach T, Pujol RM, Gallardo F, Garcia-Muret P, Climent J, Servitje O. Folliculotropic mycosis fungoides: clinicopathological features and outcome in a series of 20 cases. J Am Acad Dermatol. 2010;62:418–26.
53. Nashan D, Faulhaber D, Ständer S, Luger TA, Stadler R. Mycosis fungoides: a dermatological masquerader. Br J Dermatol. 2007;156:1–10.
54. Iorizzo M, El Shabrawi Caelen L, Vincenzi C, Misciali C, Tosti A. Folliculotropic mycosis fungoides masquerading as alopecia areata. J Am Acad Dermatol. 2010;63:50–2.